

ABSTRACT

MARTIN, JERRY HUGHES. A New Method to Evaluate Hydrogen Sulfide Removal from Biogas. (Under the direction of Jay Cheng.)

Hydrogen sulfide in biogas fuel increases the speed at which the system utilizing the biogas corrodes. This corrosion may be prevented by separating and removing hydrogen sulfide from the biogas. There are multiple technologies available to remove hydrogen sulfide (such as the gas-gas membrane tested in this thesis); however, evaluating the effectiveness of hydrogen sulfide removal in an inexpensive manner is difficult to do.

A device was constructed capable of a virtually simultaneous high precision volumetric flow and concentration measurements on moving biogas. The volumetric flow was measured by sampling the pressure from the center of two different points along a rigid tube and correlating pressure sensor voltage to the maximum velocity measured with a velocity probe. The hydrogen sulfide and methane concentrations were measured using chemical gas sensors.

A mass balance was completed around a reverse selective membrane system with the calculated difference between flows based on known input and measured output concentrations coming within 15% of each other. Though the volumetric flow measurements were in doubt, this device was able to determine that using a 20 cm² polyamide membrane under low pressures suitable for a digester (2 PSI) will increase methane concentration in biogas from 60% to 62% but is not effective at removing hydrogen sulfide.

This device was primarily designed for determining the feasibility of adapting a membrane system to a farm scale biogas generation process. This device was able to determine that using a polyamide membrane under low pressures suitable for a digester (2 PSI) will increase methane concentration in biogas from 60% to 62% but is not effective at removing 1000 ppm of hydrogen sulfide.

Keywords: Agricultural Waste, Anaerobic Digestion, Animal Wastes, Bioenergy, Biogas, Energy Recovery, Hydrogen Sulfide, Membrane, Methane, Methane Production, Selective Permeability

A New Method to Evaluate Hydrogen Sulfide Removal from Biogas

by
Jerry Hughes Martin II

A thesis submitted to the Graduate Faculty of
North Carolina State University
in partial fulfillment of the
requirements for the Degree of
Master of Science

Biological and Agriculture Engineering

Raleigh, North Carolina

2008

APPROVED BY:

Dr. D. Knappe

Dr. J. Cheng
Chair of Advisory
Committee

Dr. P. Westerman

DEDICATION

This research is dedicated to Olin and Eloise Epps (my grandparents) who sacrificed to further my education. It is also dedicated to the memory of the late Dr. William Epps (Uncle Bill) from Clemson University who inspired my work.

BIOGRAPHY

I was born in Latta, SC. My parents are Jerry Martin (an NCSU graduate) and Jane Martin. I attended Clemson University and received a bachelor's degree in electrical engineering (2003). After a brief period of working in the textile industry as a process engineer and a manager in charge of a warp-knit product line I began work on a master's degree in bioprocess engineering at North Carolina State University.

While at North Carolina State I developed virtual instrumentation for Dr Gary Roberson to teach the use of a GPS system and yield mapping. I also worked under Dr Mike Boyette developing wireless controls and monitors for bulk tobacco barns.

Near the completion of this thesis, I accepted a position working as a research engineer for the USDA-ARS Coastal Plains Research Station in Florence, SC. My position involves the development of technologies and techniques in finding new uses for biomass including alternative energy. I am involved in both biological and thermochemical technologies research.

My research interests are in bio-separations and the use of software modeling, electronic control, wireless systems and measurement technologies in microbiological systems.

ACKNOWLEDGEMENTS

There are many people who helped contribute to this research.

The original idea for this research came from a class taught by my adviser, Dr. Jay Cheng. I learned a great deal from him. My advisor and my committee Dr. Philip Westerman and Dr. Detlef Knappe held this work to high standards and forced me to push my limits further than I thought they could go.

Dr. Mike Boyette allowed the use of his lab and resources to construct the apparatus.

Deepak Keshwani, along with the rest of Dr. Cheng's research group, helped in securing supplies.

Dr. Dan Willits helped while Dr. Cheng was in Bulgaria.

Haiqing Lin from Membrane Technology and Research Inc. donated the membrane and gave technical assistance in its use.

Marcia Gumpertz and Jessie Zhang from the statistics department helped develop a statistical model. It was never used because this thesis turned into a methods thesis.

Scott Brigman of Temperance Hill, South Carolina manufactured the membrane holder at no cost.

Martin Brice from Gas Fired Products provided technical insight into the gas industry.

Cyrus Yunker helped draw up specifications for the volumetric flow sensors.

Micheal Banks from National Specialty Gases helped get the right parts to handle the corrosive gas in the apparatus.

Harold Morton with the Department of Environmental Health and Safety at NC State helped make sure this experiment was safe to run.

The building personnel, hazard response team, and firefighters responded quickly when the fire alarm was pulled. If that had been an actual gas cylinder mishap my life may have been saved.

Both the branch office of South Carolina Electric and Gas and Lockemy Scrap Metal located in Dillon SC helped with the material in some of the photos.

Dr. Keri Cantrell from USDA, agriculture research service reviewed part my thesis before I submitted it. Dr. Ro from the same location showed me how to set up the calibration curves.

Dr. George Gopen, an English professor from Duke University advised me that the most important sentence in the entire thesis was the last sentence in the first (or first group) of paragraphs. The same held true for every chapter and section. His book was helpful too. It had his research into how to produce good technical writing.

My father and mother, Jerry and Jane Martin, edited my thesis for grammatical errors.

To my parents, grandparents, and my church community I express my thanks for their patience, understanding, and support while I completed my degree.

TABLE OF CONTENTS

LIST OF FIGURES.	viii
LIST OF TABLES.	ix
CHAPTER 1 Introduction	1
CHAPTER 2 A Literature Review of Hydrogen Sulfide in Biogas	3
2.1 Introduction	3
2.1.1 Composition of Biogas.	3
2.2 The Issue with Hydrogen Sulfide	7
2.2.1 The Corrosion Phenomena	8
2.3 Methods for Eliminating Hydrogen Sulfide	12
2.3.1 Altering Anaerobic Digestion/Energy Cogeneration Process	14
2.3.2 Removing the Sulfur from Feed and Washwater	15
2.3.3 Direct Treatment of Biogas	16
2.4 Conclusion	17
CHAPTER 3 A New Method for Detecting Hydrogen Sulfide Concentration in Biogas	18
3.1 Introduction	18
3.1.1 Detecting Concentrations of Methane	18
3.1.2 Detecting Concentrations of Hydrogen Sulfide	19
3.2 Materials	19
3.2.1 Gas Sensors	20
3.2.2 Volumetric Flow Sensors	22
3.3 Methods	27
3.4 Results	27
3.5 Conclusion	33
CHAPTER 4 Testing Biogas Passed Through a Gas-Gas Membrane System for Hydrogen Sulfide Removal	34
4.1 Introduction	34
4.2 Theory	35
4.2.1 Selectivity Mechanisms	35
4.3 Materials	39
4.4 Methods	44
4.5 Data/Results	50

4.6 Conclusion	53
BIBLIOGRAPHY	55
APPENDICES	60
APPENDIX A History of Biogas	61
APPENDIX B Biogas Safety	62
B.1 Explosion	62
B.2 Asphyxiation	62
B.3 Hydrogen Sulfide Poisoning	63
B.4 Infection from Swine Wastes	63
APPENDIX C Extended Explanation for Diagrams	64
C.1 The Derivation of the Potential - pH Diagram	64
C.2 The Volumetric Flow Signal Conditioning Circuit	65
APPENDIX D Software	67
APPENDIX E Another Membrane Configuration?	72
APPENDIX F Verification of Maximum Velocity Measurement	75

LIST OF FIGURES

Figure 2.1 Breakdown of Organics into Biogas	5
Figure 2.2 Location in Cylinder Liner Where Corrosion Forms	8
Figure 2.3 Corrosion in Metal Showing Where Droplets of Electrolyte Formed	9
Figure 2.4 Pitted Anoxic Corrosion	11
Figure 2.5 Corrosion Phenomena in the Methane/Biogas-Iron System	13
Figure 3.1 Hydrogen Sulfide Sensor	20
Figure 3.2 Diagram of the Potentiostat	20
Figure 3.3 Methane Sensor	22
Figure 3.4 Circuit to Drive Methane Sensor	22
Figure 3.5 Volumetric Flow Sensing System	23
Figure 3.6 The Low Electrical Noise in the Pressure Sensing Circuit	26
Figure 3.7 Signal Conditioning Circuitry	27
Figure 3.8 Graph Comparing the Voltage of the Pressure Sensor Circuit to Maximum Velocity Over a Series of Flow Step Increases	28
Figure 3.9 The Linear Relationship between the Maximum Velocity and Pressure Sensor Voltage	29
Figure 3.10 The Signal Given When the Flow Changes from a Steady Flow of Air to a Diluted Flow	30
Figure 3.11 The Voltage Signals from the Gas Sensors when a Forty-Five Second Pulse of Biogas was added to the Diluted Flow	31
Figure 3.12 The Concentration versus the Flow Sensor Voltages	31
Figure 3.13 The Concentration Regressed on the Flow Sensor Voltage	32
Figure 4.1 The Molecular Shapes of Component Gases in Biogas	36
Figure 4.2 An Exploded View of the Membrane Holder with the Membrane in it	40
Figure 4.3 Pressurized Chamber Mounted on the Membrane Holder	41
Figure 4.4 Gas Sensors Mounted on the Apparatus	42
Figure 4.5 Close-up of Mechanisms Attached to Membrane Holder	43
Figure 4.6 Complete Apparatus	44
Figure 4.7 Diagram Showing Flows Through the Membrane	45
Figure 4.8 Thermal Correction Curve Superimposed on the Raw Voltage Curve from Flow Sensor	50
Figure 4.9 Calculation of the Input Concentrations Based on the Output Concentrations over Time	51
Figure E.1 Membrane Hanging Out Side of Holder.	73
Figure F.1 The Setup Used to Verify the Flow Measurement	75
Figure F.2 Comparing the Velocity Measurement in the Experiment to a Second Velocity Measurement Technique.	76
Figure F.3 Figure Showing the Transition from Laminar to Transitional to Turbulent Flow	77

LIST OF TABLES

Table 2.1 Composition of Various Forms of Biogas	3
Table 2.2 Stoichiometry for Sulfate Reduction and Methanogenesis	7
Table 3.1 Summary of Features of Flow Circuit	25
Table 4.1 Metrics for Biogas Quality Based on the Hydrogen Sulfide Concentration	34
Table 4.2 Properties of Component Gases Used to Select One Gas Over the Other	36
Table 4.3 Results of Final Mass Balance	52
Table B.1 Health Effects of Hydrogen Sulfide Exposure	63

CHAPTER 1

Introduction

This research addresses three economic needs of North Carolina. The first is treating wastes from the economically important swine industry, the second is for alternative fuel sources that are inexpensive, and the third is for preserving capital investments in energy conversion technologies from damage caused by sulfide corrosion.

The importance of the swine industry can be highlighted using 2004 North Carolina agricultural commodities statistics. During that year the North Carolina swine industry generated two billion dollars which accounted for over one quarter of the total revenue brought in by sale of North Carolina agricultural commodities (NCDACS, 2004). To get this revenue North Carolina housed ten million swine that excreted an estimated seven million tons of waste. Traditionally, this waste was handled using treatment system that included an open lagoon; however, a recently enacted law in North Carolina (NC law # 2007-523) has prohibited new lagoon construction. This law will force farmers to explore and improve already existing alternatives to treatment systems involving open lagoons. One of the alternatives being considered is anaerobic digestion technologies.

Anaerobically digesting swine manure is a waste management alternative with a benefit of the generation of biogas fuel. Using biogas in place of natural gas will help a farmer avoid having to buy as much gas on the open market. This protects farmers from the escalation of and volatility in natural gas prices (Wiser and Bolinger, 2007).

Most energy generation systems built to utilize biogas are constructed from metals or plastics that are vulnerable to sulfide damage. The damage to these systems begins to occur when hydrogen sulfide in biogas exceeds 100 ppm. This damage increases maintenance requirements and decreases system lifespan. Hydrogen sulfide

must be removed so having a good, inexpensive analytical test to determine the concentration and flow of hydrogen sulfide in the biogas will speed the development of better methods for reducing sulfide in biogas. This research addresses the sulfide problem by introducing a means to quickly test the effectiveness of methods that reduce the concentration of hydrogen sulfide in biogas. Having better methods for reducing biogas corrosion is likely to become more important in the coming years, especially in systems that use metals such as copper, zinc, nickel, tin, platinum, and their alloys since the supply of ore for these metals are limited (Gordon, Bertram and Graedel, 2006).

The goal of this thesis is to present an analytical technique for evaluating how well technologies work for removing hydrogen sulfide from biogas. This technique is applied to a selective gas-gas membrane system that works by pushing hydrogen sulfide through a membrane, but not methane.

The next chapter of this thesis is intended to present a thorough background of corrosion caused by biogas and current alternatives for removing hydrogen sulfide. The third chapter contains a detailed description of the development of a new analytical technique for detecting the flow and concentration of the gases in biogas. The final chapter is an analysis on a system that has the potential to effectively reduce the corrosiveness of the biogas.

CHAPTER 2

A Literature Review of Hydrogen Sulfide in Biogas

2.1 Introduction

Converting wastes into biogas is a way to recover energy from the waste, to reduce odors, to increase nutrient availability, and to reduce pathogen content (Garrison and Richard, 2005; Goodrich and Schmidt, 2002). While converting waste to biogas is desirable, one of the reasons it is not common is because of the poor quality of biogas and the high maintenance requirement of biogas using systems (Stowell and Henry, 2003). Removing hydrogen sulfide from the biogas or sulfur from any point in the biogas generation process would take care of both of these issues.

2.1.1 Composition of Biogas

Table 2.1 shows the concentration of hydrogen sulfide in biogas, as well as the concentrations of other major component gases, carbon dioxide and methane. Landfill biogas does not have as much hydrogen sulfide in it because the organic materials decompose several years while manures are digested fresh (KiHyun et al., 2005).

Table 2.1: Composition of Various Forms of Biogas

Substrate (by volume)	H_2S (ppm)	CO_2 (%)	CH_4 (%)	Source
Swine Waste	600 - 4000	40	60	(Pagilla, Kim and Cheunbarn, 2000)
Cattle Manure	600 - 7000	40	60	(Bothi, 2007)
Landfill Wastes	0 - 2000	30 - 50	50 - 70	(Shin et al., 2002)

Biogas from manure is generated biologically by anaerobic digestion of the complex organic molecules. Under anaerobic conditions microorganisms break down the organic debris until the carbon in the debris is in either its most reduced or its most

oxidized state (Kotelnikova, 2002). Roughly sixty percent of the carbon is reduced and volatilizes as methane while the rest of the carbon volatilizes as carbon dioxide (Angenent et al., 2004).

As many as 138 different microorganisms contribute to the production of biogas from swine manure with the majority of them being strict anaerobes (Iannotti, et al., 1982). As presented in Figure 2.1, these microorganisms can be broadly classified into two physiologically distinct groups. The first group breaks down the complex organics into simpler organic molecules (hydrolytic and fermentor organisms). The second group uses the simple organic molecules, particularly acetate and hydrogen, to make methane (methanogenic organisms) (Cappenberg, 1975; Tchobanoglous, et al, 2002).

While manure is being digested, very small bursts of hydrogen sulfide will bubble out (Ni et al., 2001; Arogo et al., 2000) and accumulate as a small portion of biogas. Hydrogen sulfide is produced during hydrolysis when certain organisms break down the essential amino acid methionine (Ravanel et al., 1998; Zhu, et al., 1999). In the methanogenic stage hydrogen sulfide production continues because a different group of sulfate reducing organisms can use fatty acids, particularly acetate, as a substrate (Tchobanoglous, et al., 2002).

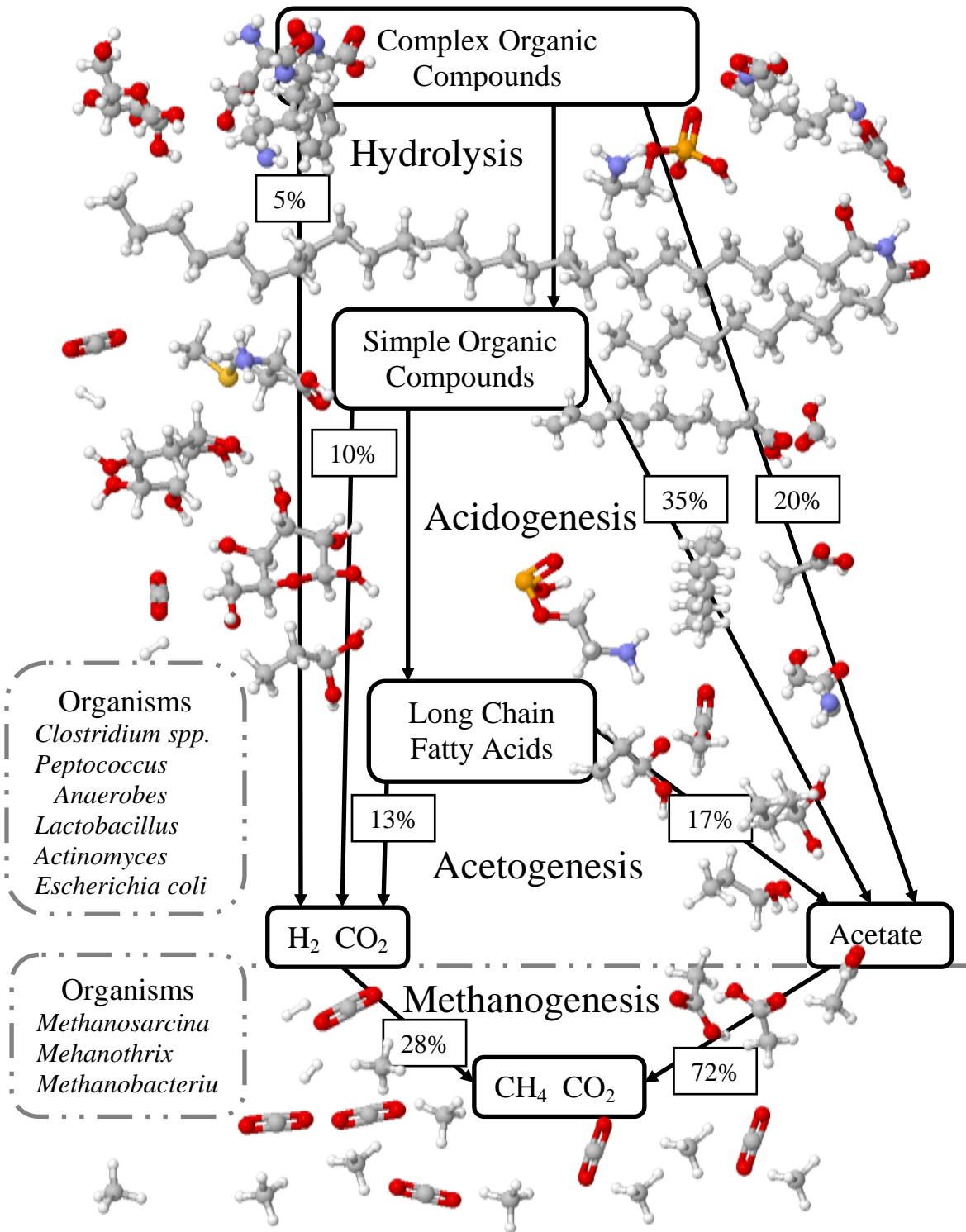


Figure 2.1: Breakdown of Organics into Biogas

Sulfate reducers are a nuisance because they grow faster than methanogenic organisms using the same substrates (Oremland and Polcin, 1982). This was shown when acetate and sulfate were used to culture a sulfate reducer *Desulfobacter postgatei* and a methanogen *Methanosarcina barkeri* with similar maximum growth rates, μ_{max} . The half saturation coefficient, K_s , for *Desulfobacter postgatei* was 0.2 mM which was fifteen times less than *Methanosarcina barkeri*'s K_s which was 3 mM (Schönheit, Kristjansson and Thauer, 1982). Acetate concentration in swine manure is around 51 mM (Hansen, Angelidaki and Ahring, 1999) so the growth rate, μ , can be calculated as a percentage of μ_{max} using the basic growth model in equation 2.1. μ for methanogens is 94% μ_{max} while μ for the sulfate reducers is 99.6% μ_{max} . In a batch process μ for the methanogens drops off quickly as acetate is consumed.

As sulfate is reduced hydrogen sulfide is formed, which is another problem because the hydrogen sulfide byproduct is inhibitory to all organisms involved in anaerobic digestion (Cypionka, 1986), especially the methanogens (Hulshoff et al., 1998, Chen et al., 2008).

$$\mu = \frac{\mu_{max} \cdot S}{K_s + S} \quad (2.1)$$

When conversion techniques other than anaerobic digestion are used, hydrogen sulfide is still a problem. A gas similar to biogas called syngas can be produced from manure by gasification or pyrolysis using a thermochemical reactor (Chang, 2004). Thermochemical reactors use more energy than anaerobic digesters, however, they are more compact and convert the waste much faster (Cantrell et al., 2007). During thermochemical conversion, syngas is created by heating up the manure in either completely or partially anoxic conditions. When heated the manure reduces to a

combination of hydrogen gas and carbon monoxide. This gas can be reformed into methane and carbon dioxide by passing it through high temperature steam. In thermochemical reactions free energy changes tend to favor sulfate reduction over methane formation. Table 2.2 shows the free energies associated with different sulfate reductions.

Table 2.2: Stoichiometry for Sulfate Reduction and Methanogenesis

Reaction	ΔG (kJ/mol)
Sulfate-reducing reactions	
$4H_2 + SO_4^{2-} + H^+ \rightarrow HS^- + 4H_2O$	-38.1
$Acetate^- + SO_4^{2-} \rightarrow HS^- + 2HCO_3^-$	-47.6
$Propionate^- + \frac{3}{4}SO_4^{2-} \rightarrow \frac{3}{4}HS^- + Acetate^- + HCO_3^- + \frac{1}{4}H^+$	-37.7
Methanogenic reactions	
$4H_2 + HCO_3^- + H^+ \rightarrow CH_4 + 3H_2O$	-33.9
$Acetate^- + H_2O \rightarrow CH_4 + HCO_3^-$	-31.0

adapted from Lens et al. (1998)

2.2 The Issue with Hydrogen Sulfide

Hydrogen sulfide in biogas is one of the main reasons that the benefits currently do not outweigh the cost of an anaerobic digester (Garrison and Richard, 2005; Stowell and Henry, 2003). There are a few cases, such as one dairy waste digester reported by Goodrich and Schmidt (2002), that had few problems in terms of hydrogen sulfide damage, but in most cases the damage from the sulfide in the biogas causes equipment and maintenance costs to increase (Li, 1984; Lusk, 1998). Picken and Hassaan (1983) explicitly mention engine problems caused by hydrogen sulfide in biogas when it is burned as a fuel.

Biogas from anaerobic digestion is mostly methane. If biogas were pure methane it would be an excellent choice for a fuel. Methane has a simple structure and is highly stable, which allows for ease of storage and handling. As an engine fuel it has the advantages of complete combustion, no dilution of lubricants, better exhaust performance, and good anti-knock properties (Jiang, et al., 1989). Biogas, however, is only sixty percent methane. The remaining forty percent is mostly acid gases (primarily carbon dioxide) with hydrogen sulfide causing the most problems. When real biogas is burned as a fuel engines tend to wear out quickly. Picken and Hassaan (1983) have shown that the first part of a biogas engine to wear out is the cylinder liner at the upper position of the piston ring (see figure 2.2). Excessive wear in cylinder liners at this position is caused by the corrosion phenomena (Sudarshan and Bhaduri, 1983; Goode, 1989).

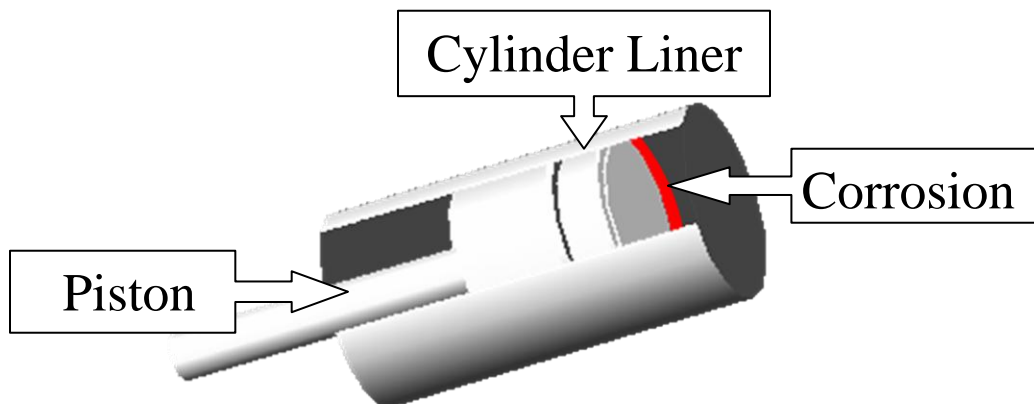


Figure 2.2: Location in Cylinder Liner Where Corrosion Forms

2.2.1 The Corrosion Phenomena

Corrosion is the degradation of a metal as it is converted from a desired to an undesired form. All metals corrode at certain electrochemical and thermodynamic conditions. These conditions depend on the pH, chemical potential, and temperature of the solution. When corrosion occurs, metal ions dissolve into a solution releasing

electrons into the metal that is left. These electrons are conducted through the metal to a location where the solution, metal, and possibly atmosphere meet. There the electron is accepted by any oxidizing agent present. In this research the common oxidizing agents that form stable corrosion compounds with the metal are oxygen and sulfur. As more metal ions dissolve and are oxidized the parts that are metal will become damaged by being eaten away or by converting into a material resembling the metal's ore (Hamilton, 1985). (See equations 2.2, 2.3, and 2.4) Figure 2.3 shows where droplets of solution formed on the surface of the metal.

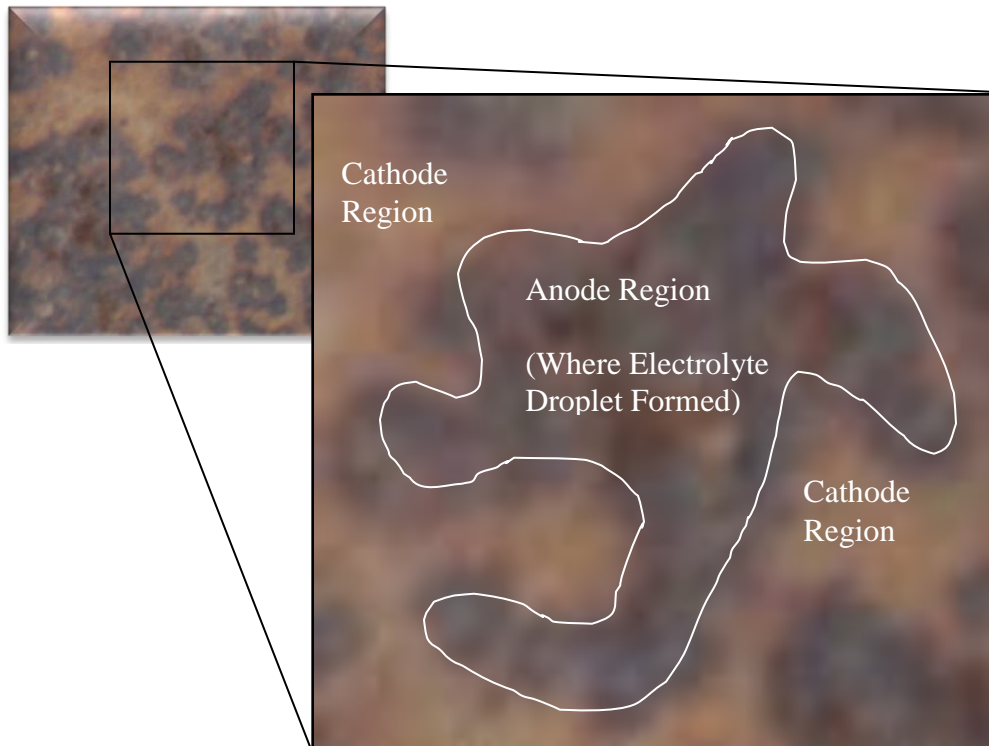
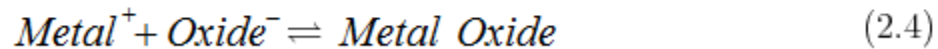
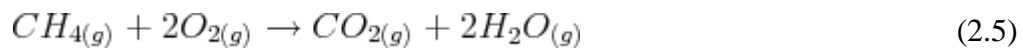


Figure 2.3: Corrosion in Metal Showing Where Droplets of Electrolyte Formed

Corrosion occurs during normal methane combustion. Assuming standard conditions, combustion of 1 liter of methane (see equation 2.5) has the potential to produce 1.4 ml of liquid water and 0.9 liters of carbon dioxide. (In industry standard units 100 ft³ of methane has the potential to produce 1.0 gallons of liquid water and 91 ft³ of carbon dioxide.) The water produced is an electrolyte and the oxygen is the oxidizing agent needed for corrosion. The carbon dioxide speeds up the corrosion by making the electrolytic solution more acid which, in turn, speeds up the dissolution of the metal into ions.



Hydrogen sulfide is oxidized into sulfur dioxide which dissolves as sulfuric acid. Sulfuric acid, even in trace amounts, can make a solution extremely acidic. Extremely acidic electrolytes dissolve metals rapidly and speed up the corrosion process. This is particularly true in high temperatures, such as is the case with the afore mentioned cylinder liner.

Even if there is no oxygen present, biogas can corrode metal. Hydrogen sulfide can become its own electrolyte and absorb directly onto the metal to form corrosion. (Brown, 2004). If the hydrogen sulfide concentration is very low, the corrosion will be slow but will still occur due to the presence of carbon dioxide. People in the pipeline industry refer to this type of corrosion as sweet corrosion which is recognized by very deep pits (Smith, 1993). The mechanism for this reaction is given in equations 2.6-2.8 (López, Pérez and Simison, 2003). If the concentration of hydrogen sulfide in the gas is greater than 100 ppm, people in the pipeline industry refer to the corrosion as sour corrosion which is recognized by pits as shown in figure 2.4 (Smith, 1993). This mechanism is given in equation 2.9.

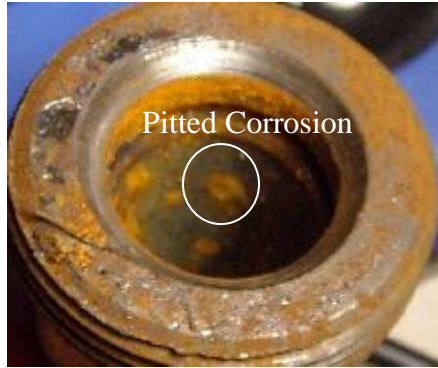
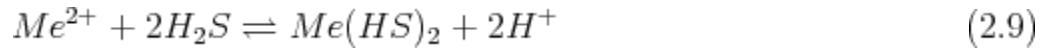
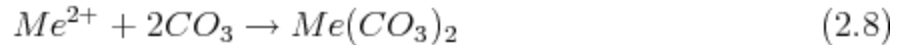
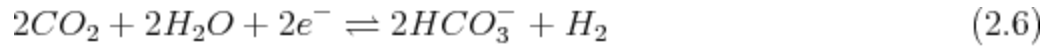


Figure 2.4: Pitted Anoxic Corrosion

The presence of hydrogen sulfide causes metals to become more active. Describing a metal as active is one of three ways to describe the resistance of a metal to corrosion given a certain set of thermodynamic conditions. The other two are immune and passive. Immune metals, for example gold, have natural nobility but are too expensive for making systems that handle biogas. Passive metals are typically used in biogas applications. These metals have an oxidized coating that slows corrosion. Active metals have no resistance to corrosion and will dissolve on contact with an electrolyte. Anything that makes a metal more active will make it corrode faster.

The potential - pH diagram, also known as a Pourbaix diagram, is a graphical way to show the effect of hydrogen sulfide on the corrosion of metal parts. Figure 2.5 is a potential - pH diagram for a biogas - iron corrosion system at standard conditions. Though metal systems for using biogas are never made of pure iron, the pure iron system has similar thermodynamics, more simplicity, and more empirical data to back it up than the carbon-iron (steel) or carbon-chromium-iron (stainless steel) typically used

in the construct biogas burning systems. The derivation of this diagram is in appendix C.1.

Point one in figure 2.5 describes the pH and potential a water droplet would have in standard conditions for a pure methane-iron system. Adding air to the system shifts the pH and potential of the water droplet from point one to point two. The speed of corrosion increases as air is added, but this effect is counteracted because the iron will become passive, or form a protective oxide coating. The difference between the water droplet in the iron-methane system and the iron-biogas system is shown by shifting from point one to point four. This shift causes a slight increase in the speed of corrosion. The practical scenario for utilizing biogas is a shift from point one to point three, where the biogas is used and oxygen is present. In this scenario the corrosion is fast and the oxide coating is not as stable, which causes pits form and drastically reduces the useful life of the metal.

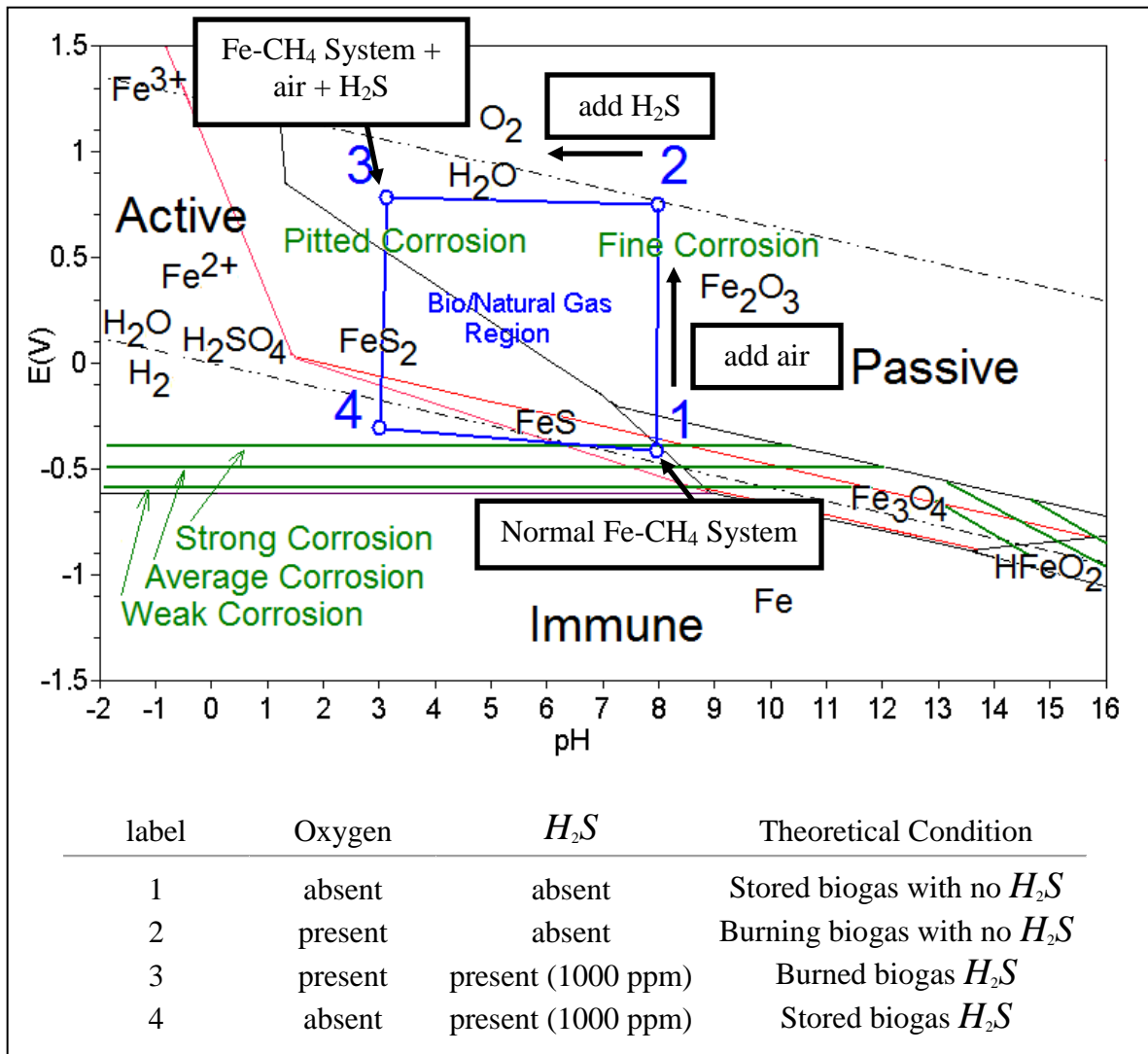


Figure 2.5: Corrosion Phenomena in the Methane/Biogas-Iron System

2.3 Methods for Eliminating Hydrogen Sulfide

The main problem with hydrogen sulfide is that it speeds up corrosion. Corrosion of metals occurs naturally in devices that burn methane. Trace amounts of hydrogen sulfide in the gas makes the corrosion worse. For this reason it is hard to use

biogas to displace natural gas without first removing the hydrogen sulfide. There are several methods currently available for removing the sulfide gas.

2.3.1 Altering Anaerobic Digestion/Energy Cogeneration Process

Codigestion

Codigestion refers to digesting multiple substrates in a digester simultaneously. The main benefit of codigestion is the ability of neutralizing two different types of waste in one digester (Pesta, 2006). There is evidence to suggest adding food wastes to dairy waste digesters has reduced the concentration of hydrogen sulfide (Bothi, 2007). The major problem is that both materials must be available at the same site in the right quantities, which is a rare occurrence. If this is not the case transportation costs may be involved.

Digester Additions

Iron chlorides, phosphates, and oxides can be added directly to the digester to bind with the sulfides in the digester and make them insoluble. The addition of iron III phosphate has been observed to reduce hydrogen sulfide concentration (McFarland and Jewell, 1989). This solution involves costs of the additions.

Multiple Phase Digestion

Typically, multiple phase digestion improves the speed of degradation and the stability of the process. This is done by having one chamber of a digester for the complex organics to be broken down (the hydrolysis phase of digestion) and a second chamber for the simpler organics to be broken down (the methanogenesis phase). The biogas from the first phase is treated and released. This gas contains about 90% carbon dioxide and most of the trace gases, including most of the hydrogen sulfide found in biogas (Pesta, 2006). A two phase digester as reported by Pagilla, et al. (2000)

experimentally verified this result holds true for swine waste biogas by generating biogas with 300 ppm hydrogen sulfide.

Buffering the pH

Buffering pH in the reactor is one way to control the contents of biogas being released. Different pH levels may destroy enzymes or alter the chemical equilibriums of bioreactions within the digestion process (Pesta, 2006). Increasing the reactor pH from 6.7 to 8.9 will decrease the sulfide production from 2900 ppm to 100 ppm (McFarland and Jewell, 1989). However, increasing the pH increases the concentration of free ammonia which is inhibitory to methanogenesis.

Frequently Changing Engine Oil

Frequently changing the oil in an engine is a simple way to control corrosion. Changing the oil takes advantage of the mechanism built into an engine to limit the corrosion of the metal parts (Bothi, 2007). The disadvantages of this method are that it is labor intensive and costly.

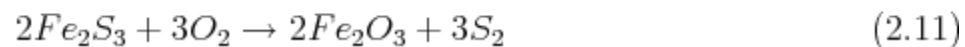
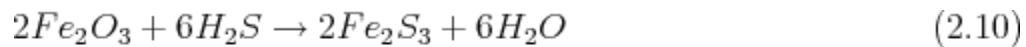
2.3.2 Removing Sulfur from Feed and Washwater

The sulfur enters in the farm through the protein in the feed. Removing protein from the feed is not a practical solution because farmers tend to optimize feeds for product yields and animal health. In certain regions sulfates can be eliminated from the animal drinking water. Another approach is to prevent any material with a high sulfate concentration from getting into the digester. Using high sulfur content wash waters has been observed to raise the hydrogen sulfide levels in biogas considerably (Bothi, 2007).

2.3.3 Direct Treatment of Biogas

Sorptive Media

Sorptive media are materials placed in the path of the biogas that react with the corrosive gasses within the biogas. Most sorptive media use some form of metal oxide, of which the most common is iron sponge. The iron sponge reaction is given in equation 2.10 - 2.11. Other metals that may be used are zinc and sodium.



Other media that can sorb hydrogen sulfide include zeolites and activated carbon. Coating these media with alkaline solutions has been done to neutralize hydrogen sulfide gas. The primary disadvantage of absorptive media is that the media needs to be replaced or recharged after a certain period of time.

Wet Treatments

Wet treatments are generally not preferred for treating gas going into an engine because water must be removed after the treatment. Wet treatments include treatments using metal oxide, chelated iron, quinone, vanadium, nitrite, alkaline salts, amine solutions, and solvents. These treatments typically have a high initial costs and maintenance costs. The most economical of these treatments is probably chelated iron. These treatments are usually found in natural gas refineries as opposed to farms because of the high equipment costs. Some of these treatments involve a high cost, non-regenerable reactant.

Biological Treatments

Biological treatment of hydrogen sulfide typically involves passing the biogas through biologically active media. These treatments may include open bed soil filters, biofilters, fixed film bioscrubbers, suspended growth bioscrubbers and fluidized bed

bioreactors. These filters rely on the biological oxidation of the hydrogen sulfide in the biogas and are ideal for treating the swine waste gas before it is released into the environment (Nicolai and Janni, 1997). However, biological media works best when wet, so moisture has to be removed before burning biogas in an energy generation process.

2.4 Conclusion

Converting swine wastes into fuel as a means to recover its energy content has promise, but the sulfur must be removed at some point in the biogas generation process. Removing sulfur from feed or wastes is difficult so removing the sulfide straight from the biogas may be the best method of dealing with the problem. A good method to test for the removal of sulfide will be useful as the technology of converting swine wastes into biogas continues to be developed.

CHAPTER 3

A New Method for Detecting Hydrogen Sulfide Concentration in Biogas

3.1 Introduction

The effectiveness of hydrogen sulfide removal in biogas is determined by measuring the volumetric flow of hydrogen sulfide. To measure the volumetric flow of hydrogen sulfide in biogas, the bulk volumetric flow of the biogas and concentration of hydrogen sulfide in the gas are detected virtually simultaneously using an electronic system. An electronic sampling system allows a large number of samples to be taken and complex filtering algorithms to be used to reduce the noise and to improve the accuracy of the measurement. These measurements can be recorded so the nature and transient behavior of the movement of hydrogen sulfide can be determined.

3.1.1 Detecting Concentrations of Methane

The first commercially available methane sensors were produced in the 1920's to detect explosive gases in mines. These gases would cause a slight deflection in voltage across two electrodes that could be detected and amplified with electronic hardware available during that time. In the 1960's the methane gas sensor developed rapidly in response to many explosions occurring after the popularization of bottled LPG gases (Ihokura and Watson, 1994).

Today, one of the best sensors available to detect methane is a tin oxide, sometimes referred to as a stannic oxide, sensor. These sensors are constructed by embedding a heating element and two electrodes into a tin oxide plate. Unlike most electrolytic cells, all of the electrodes are chemically inert. Tin oxide is an n-type semiconducting material which means there are free electrons in the material. A reducing gas reacts with oxygen within the tin oxide and consumes it. This reaction

reduces the free electron mobility which causes the resistance of the material to increase. The change in resistance is proportional to the log concentration of the gas present (Watson et. al., 1993).

Most combustible gases like carbon monoxide, hydrogen, or methane are reducing gasses that will increase the resistance of the material. Selectivity (or the ability to detect the correct gas) of the sensor is modified by changing the temperature of the tin oxide plate. Higher temperatures will cause carbon monoxide and hydrogen to react quickly at the surface, while the more chemically stable methane can penetrate deeper into the sensor to react. These quick reactions at the surface of the sensing plate will prevent the tin oxide sensor from being as sensitive to hydrogen and carbon monoxide (Watson et al., 1993). This mechanism prevents the sensor from detecting hydrogen sulfide as well (M.Gaidi and Labeau, 2000).

3.1.2 Detecting Concentrations of Hydrogen Sulfide

Most hydrogen sulfide sensors available today use a potentiostat circuit. Potentiostats have been around since Alessandra Volta pioneered the electrochemical series in the late 1700's. A breakthrough was reached when Hickling developed the first automatic potentiostat using vacuum tube based thyratrons and other electronics available in the early 1940's (Hickling, 1942). Since the development of the miniaturized electronics, hydrogen sulfide sensors relying on transistor based technology have been developed to detect hazardous concentrations of hydrogen sulfide (Moseley, 1997). These sensors are primarily used in the natural gas, petroleum, wastewater, and pulp and paper industries.

3.2 Materials

The entire apparatus was mounted on a 2.3 m by 1.2 m (8' x 4') sheet of plywood which was strapped to a wheeled cart. Biogas for this experiment was simulated using a pressurized gas cylinder which was fastened to the plywood. The

gas was sixty percent methane, 1000 ppm hydrogen sulfide and balanced with carbon dioxide. A stainless steel regulator regulated the pressure of the gas.

3.2.1 Gas Sensors

Hydrogen Sulfide Sensor



Figure 3.1: Hydrogen Sulfide Sensor

The three terminal 4HS/LM Cititech sensor head (shown in figure 3.1) detected the hydrogen sulfide. Inside the sensor head the three terminals were attached to a sensing, counter, and reference electrode suspended in a liquid electrolyte. The electrolyte was immobilized within the sensor head by a diffusion barrier that allowed hydrogen sulfide to pass. Externally the three electrodes were attached to a potentiostat circuit as shown in figure 3.2.

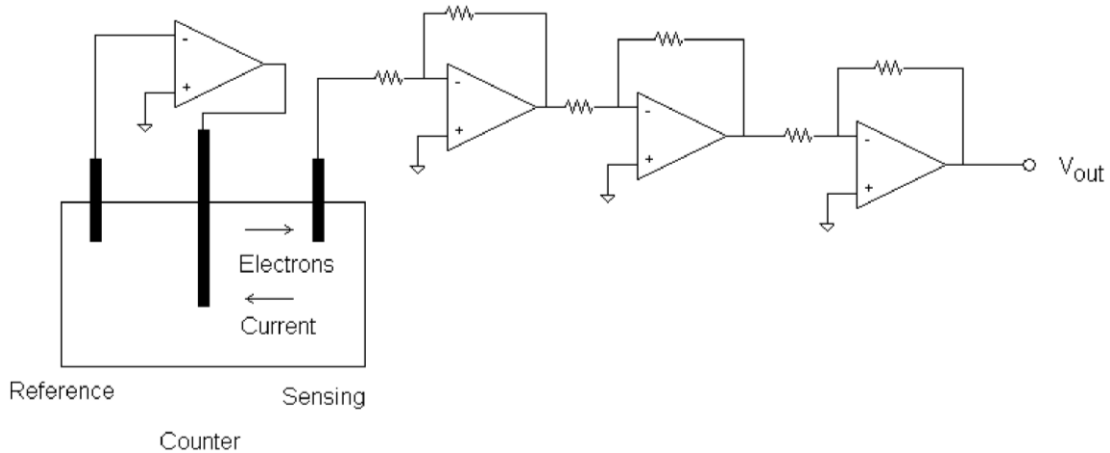
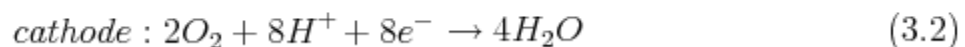
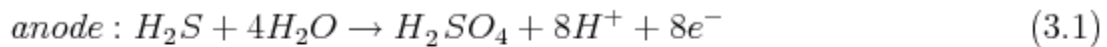


Figure 3.2: Diagram of the Potentiostat

The potentiostat works by using a voltage to drive a normally corrosion prone electrode into immunity and measuring the current required to maintain that immunity. The hydrogen sulfide causes a reaction to occur at the anode (reference electrode) that under most circumstances would corrode the anode and release electrons (See equation 3.1) flowing toward the cathode (sensing electrode) where a counter reaction would occur (see equation 3.2). In a potentiostat the movement of electrons is stopped by an op amp in an open loop configuration that forces a specified voltage difference between the anode and the counter electrode. Theoretically, no current passes through the anode (reference electrode) which prevents the anode from corroding. The op amp draws current from the solution through a third electrode (counter electrode). This current causes a voltage difference proportional to the hydrogen sulfide concentration in the electrolyte between the sensing and the counter electrode. Since the counter electrode is not an anode prone to corrosion, this signal is stable.

The small voltage difference generated in the potentiostat is measured with a 10 ohm voltage divider and a high gain three stage junction field effect transistor (JFET) amplifier circuit. This circuit measures hydrogen sulfide up to 100 ppm and the maximum overload is 500 ppm. This signal is about 0.15 uA/ppm with a sensitivity of 0.1 ppm. In less than five seconds this sensor will react to the presence of hydrogen sulfide.



Methane Sensor

A MQ-5 Hanwei sensor head, as shown in figure 3.3, was used to detect methane. The resistance of this sensor varied with the log concentration of methane. A voltage divider converted the resistance into a voltage (see figure 3.4). A voltage follower transformed the impedance of the signal from the voltage divider to prevent

loading when the signal went to the data logger. In less than 10 seconds these sensors can measure from 1-10% methane.



Figure 3.3: Methane Sensor

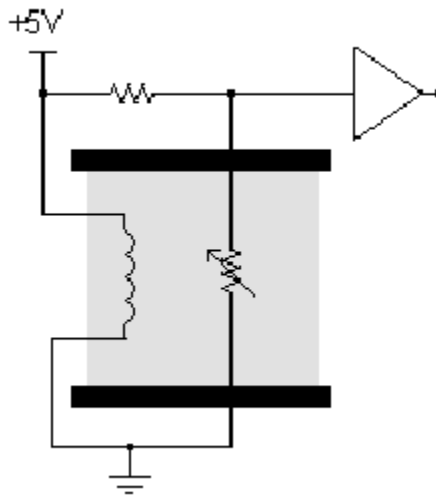


Figure 3.4: Circuit to Drive Methane Sensor

3.2.2 Volumetric Flow Sensors

The gas sensors used in this experiment were developed to detect hazardous concentrations of gas. Because both types of sensors were designed for use in the atmosphere, they rely on the presence of atmospheric oxygen to work. Thus it is necessary to dilute biogas with air for concentration sensors to work. For safety reasons, the dilution ratio used in this experiment was less than one part biogas to forty parts air. One part biogas to ten parts air was avoided because at that ratio the flash point of the biogas - air mixture dropped low enough for the gasses to explode.

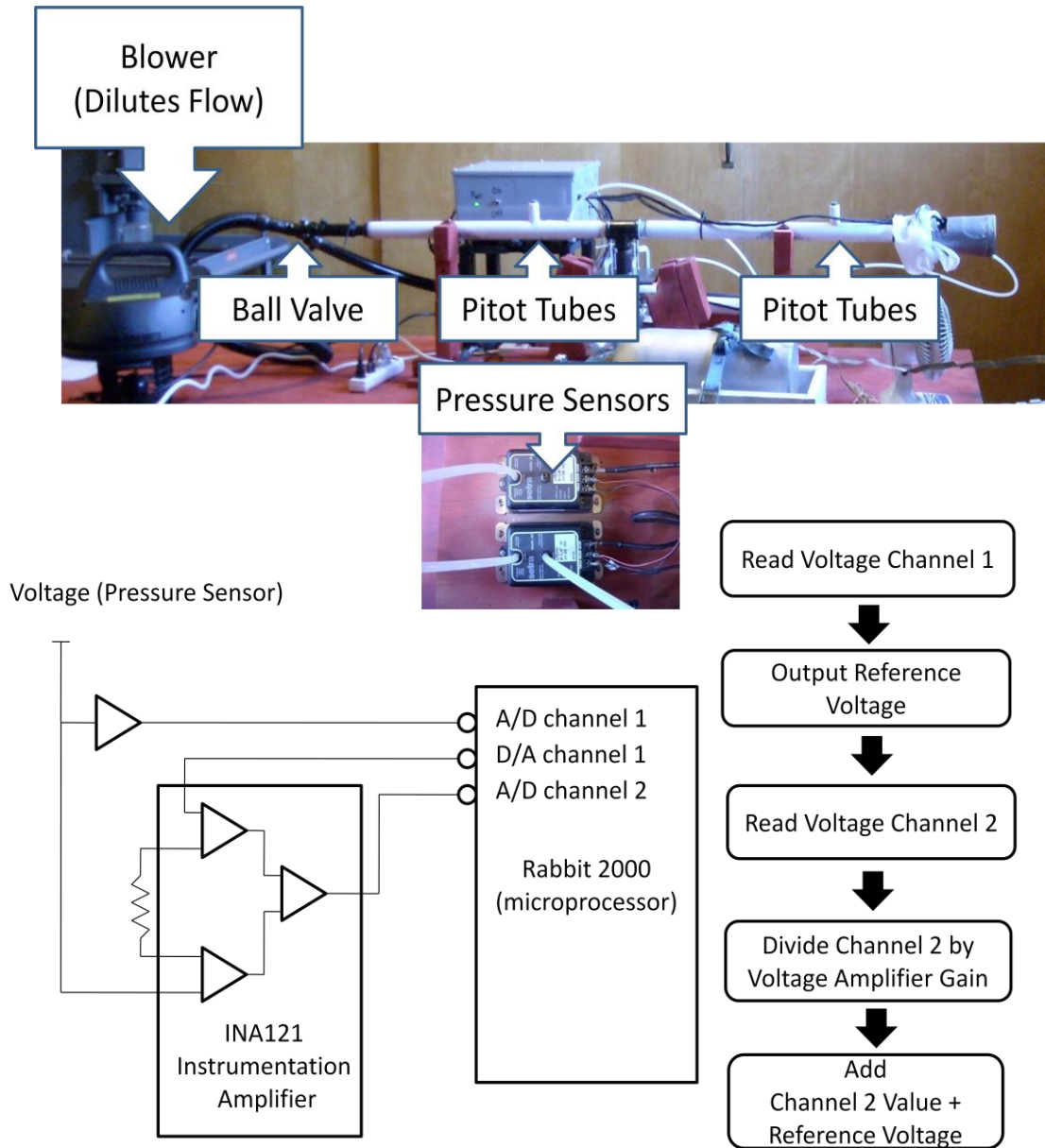


Figure 3.5: Volumetric Flow Sensing System

The system shown in figure 3.5 was designed to measure the volumetric flow of the diluted biogas. This system was designed to handle corrosive biogas and measure small changes in the diluted flow. Going from left to right at the top of figure 3.5, dilution air was supplied from a shop vacuum cleaner configured as a blower. A ball

valve was used to regulate the airflow going into two rigid, smooth walled, two meter (six foot) fiberglass tubes with a diameter of 2.54 cm (1 in). The tubes had a distance roughly eleven times the diameter before and three times the diameter after each measuring point. This was so the flow would take on the characteristics of a slow, incompressible Poiseuille flow with a parabolic velocity profile at each of the sampling points.

The biogas was released into the middle of these tubes between the two sampling points. One pitot tube was placed at a sampling point before to location the biogas was injected into the tube and another was placed at a sampling point after the biogas was injected. The pitot tubes were oriented vertically and pointed into the middle of the flow. The height of the pitot tube was adjusted until the signal was maximized from an attached Setra model 264 differential pressure sensor (middle of figure 3.5.) The deflection of a stainless steel membrane within the sensor was used to measure the difference in pressure between the two points.

The pressure difference (ΔP) was directly proportional to the volumetric flow (Q). This relation is evident in the Poiseuille equation (equation 3.3) which relates pressure change through a tube to dynamic viscosity (μ) of the fluid, the effective length between the pitot tubes (L), and effective radius of the tube (r) for a laminar flow. This equation could not be used directly to calibrate the apparatus because of how apparatus was built. There was a severe constriction of the tube at the location where biogas was injected. This constriction aided in the mixing of the gasses, but it caused too much of a pressure drop at that point for the Poiseuille equation to be useful. The Poiseuille equation is still useful to show that there is a relation between the pressure difference and the volumetric flow and more importantly that the pressure difference can be used to measure the volumetric flow.

$$\Delta P = \frac{8\mu L Q}{\pi r^4} \propto Q \quad (3.3)$$

The voltage signal from the pressure sensor was recorded on a data logging circuit. A specialized circuit (bottom of figure 3.5) was built to measure the pressure sensor voltage with a sensitivity in the millivolt range and all the electrical noise attenuated. Table 3.1 lists the features that were needed to attenuate the noise. This table is fully explained in section C.2 in the Appendix.

Figure 3.6 is the quiescent output of the flow measuring circuit with the ability to attenuate the normally 20 mV thermal noise to less than 1 mV before sending the signal to the data logger. As evident in figure 3.6 there was no biasing circuitry built into this system so the average quiescent voltage is not exactly zero volts.

Table 3.1: Summary of Features of Flow Circuit

Feature	Reason Used	Issue Addressed
JFET op-amps	extreme input impedance	flow sensor loading
switching power supply	well regulated supply	variation in loading
analog and digital supply separation	no power supply crossover	noise from processor
reference point supplied by the software	no reference point crossover	floating ground
shielded sensor cable	grounds EM noise	electromagnetic signals
twisted pair sensor cable	Cancels cable inductance	crosstalk
solid copper sensor cable	low impedance	loading effect of cable
100 samples per ten second averaging filter	high frequency filter with no distortion	thermal noise that cannot be eliminated from circuit

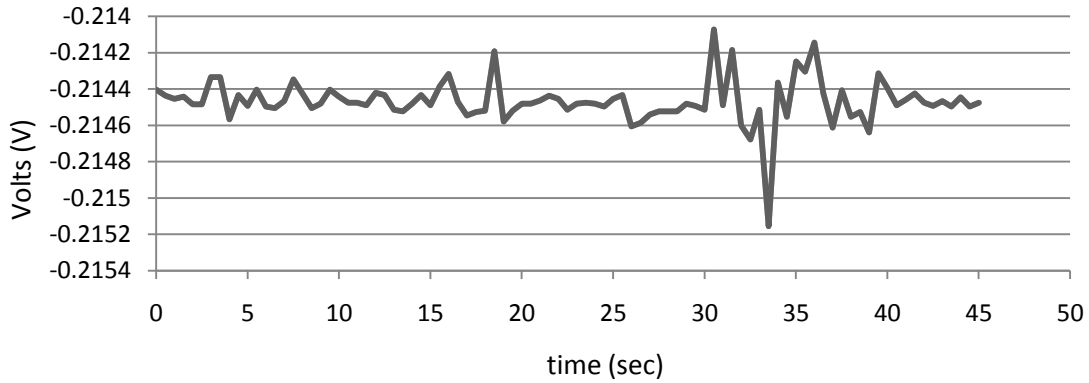


Figure 3.6: The Low Electrical Noise in the Pressure Sensing Circuit

The processor used for data logging was a rabbit 2000 on a wildcat BL2000 motherboard manufactured by Rabbit Semiconductor. The software was programmed in Dynamic C++ using ANSI C programming conventions. The code to run the device is given in appendix D. The main purpose of the software was to take measurements from the three types of sensor circuits tied to the A/D channels, which were the flow circuit and the two gas sensor circuits. The software also managed the voltage of the reference point on the flow sensors. The electrical system is shown in figure 3.7.

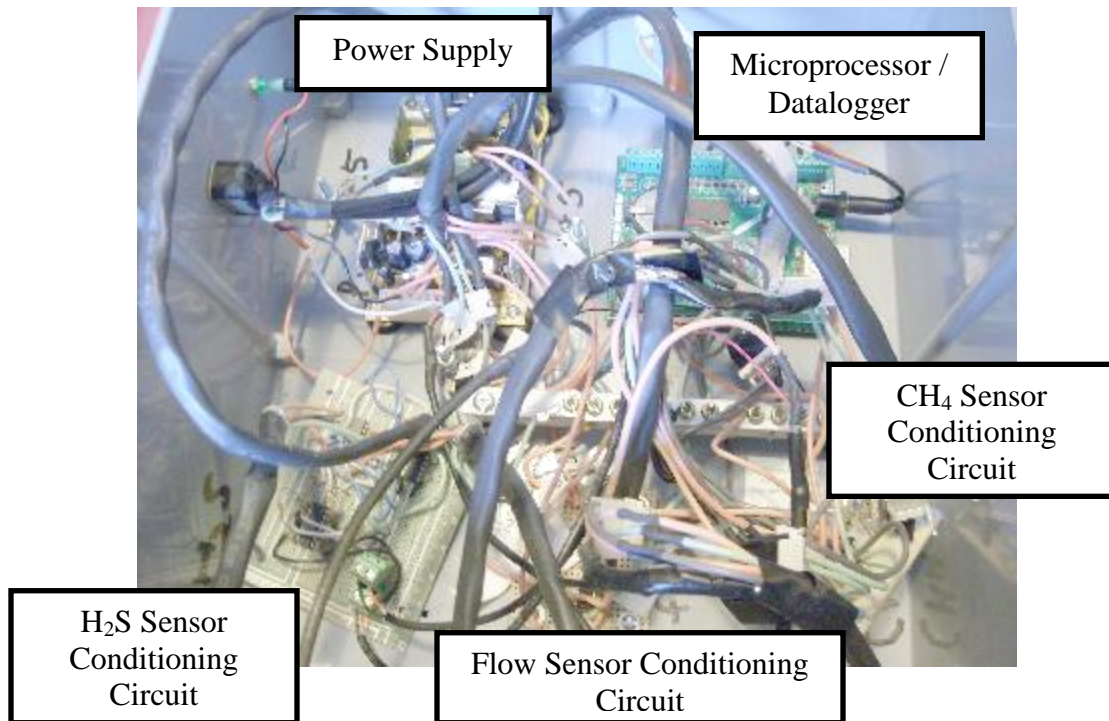


Figure 3.7: Signal Conditioning Circuitry

3.3 Methods

Each of the sensors were tested for interference from other gasses (cross-sensitivity). The hydrogen sulfide sensor was tested for cross sensitivity using an injection of methane gas. The methane sensor was tested using hydrogen sulfide prepared by reacting sulfur and steel wool with heat and then adding hydrochloric acid. The sensors were tested for carbon dioxide using a vinegar and baking soda reaction. The cross sensitivity was negligible in both types of gas sensors.

3.4 Results

The voltage signal from the Setra pressure sensors was converted into a maximum velocity signal using a calibration curve. The calibration curve was generated using data recorded by the pressure measurement circuit while measuring a series of step increases in flow. At each of the flow steps the maximum velocity (or

the center velocity) of the air leaving the tube was recorded with a Seirra Instruments 610 Flo-meter (air velocity meter) with an Accu-Flo™ self-heated platinum resistance temperature deflector. The signal from the Setra sensors is plotted against time in figure 3.8 with the maximum velocity measured from the Seirra air velocity meter recorded at each step.

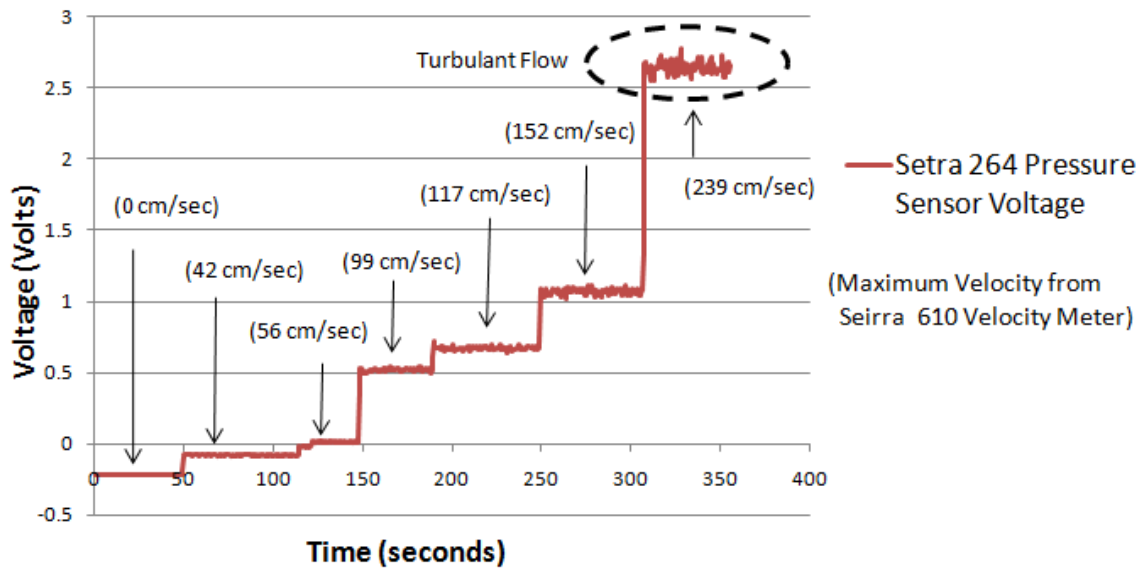


Figure 3.8: Graph Comparing the Voltage of the Pressure Sensor Circuit to Maximum Velocity Over a Series of Flow Step Increases

Most of the flow measurements were laminar. The effects of turbulence were evident at 239 cm/sec on both the curve in figure 3.8 and on the Seirra air velocity meter. For the flows not affected by turbulence (laminar flows) a characteristic equation relating the maximum velocity to the voltage from the pressure sensors was developed (see figure 3.9.)

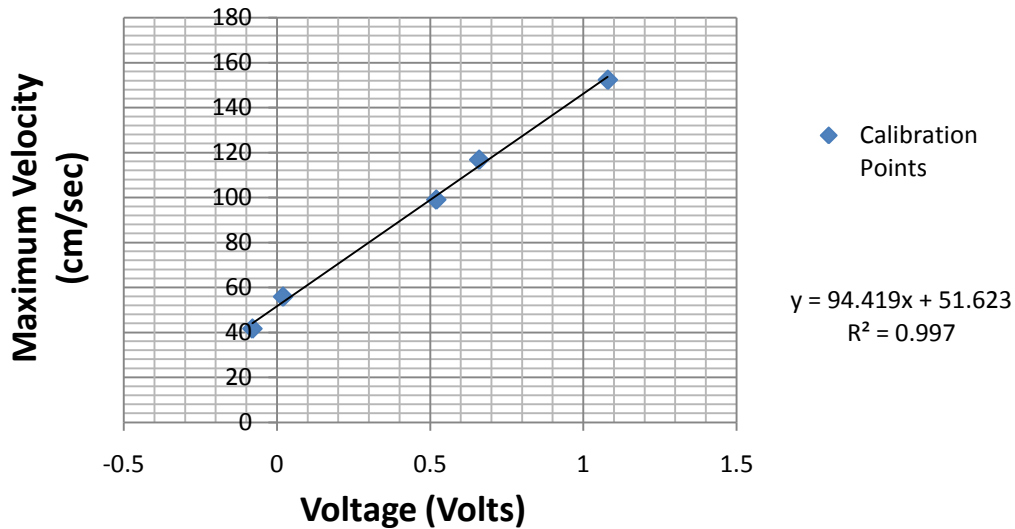


Figure 3.9: The Linear Relationship between the Maximum Velocity and Pressure Sensor Voltage

The laminar range of maximum velocities measured by the pressure sensors was from 40 to 160 cm/sec and the resolution was less than 0.1 cm/sec. The resolution was based on the standard deviation from the mean flow signal.

The maximum air velocity measured in the laminar flow was converted to an average air velocity by dividing the maximum by two. The laminar flow was verified by observing turbulence on both the pressure sensors and air velocity meter. The flow was further verified by cross checking with a WE Anderson prandtl tube and Alnor 560 monometer. (The data for these measurements are in appendix F.) The average velocity was converted into a volumetric flow rate by multiplying by the cross-sectional area of the tube.

For the concentration sensors, a similar calibration curve was developed. Before these sensors would work they had to remain powered for twenty-four hours to reach chemical equilibrium. The valve on the cylinder with the simulated biogas was opened releasing a step input of biogas into the airflow within the tubes. This gas deflected the

voltage of the Setra pressure sensors. Figure 3.10 shows such a deflection occurring between twenty and one hundred seconds.

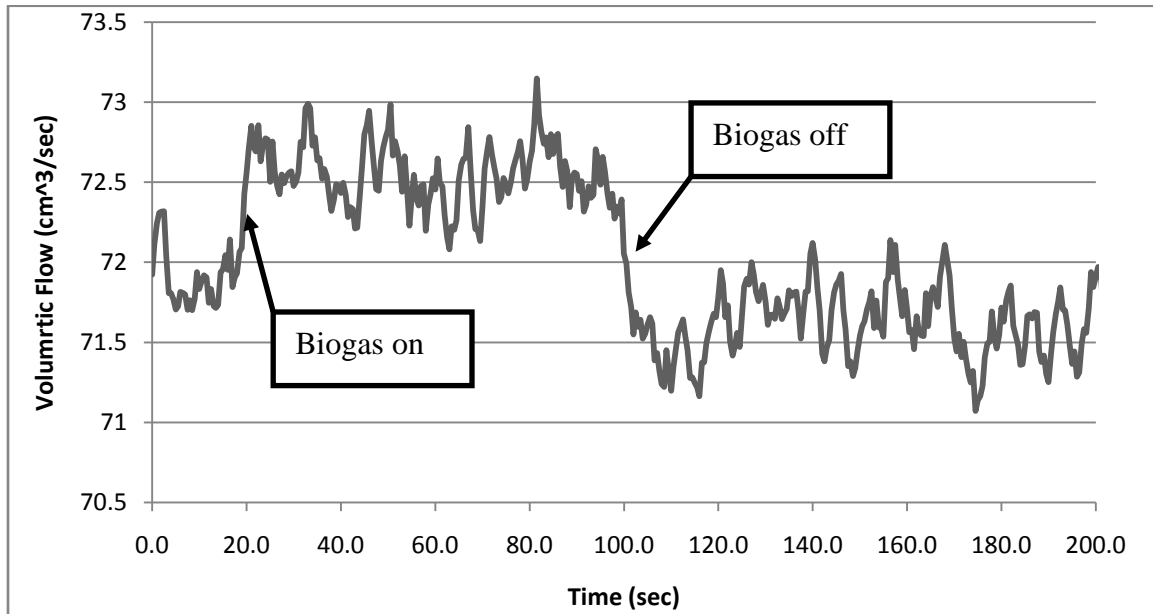


Figure 3.10: The Signal Given When the Flow Changes from a Steady Flow of Air to a Diluted Flow

The slight change in volumetric flow when the step input of biogas was diluted in the flow through the tube was measured. Because the initial concentrations of hydrogen sulfide and methane in the biogas were known, it was possible to calculate the concentration of the biogas in the diluted flow. The deflection of the voltage in the gas sensing circuit when a forty five second pulse of biogas was added (see figure 3.11) was used relate the voltages of the gas sensing circuit to the concentration of the component gas concentrations in the biogas. This was repeated using different flow rates of the simulated biogas (see figure 3.12).

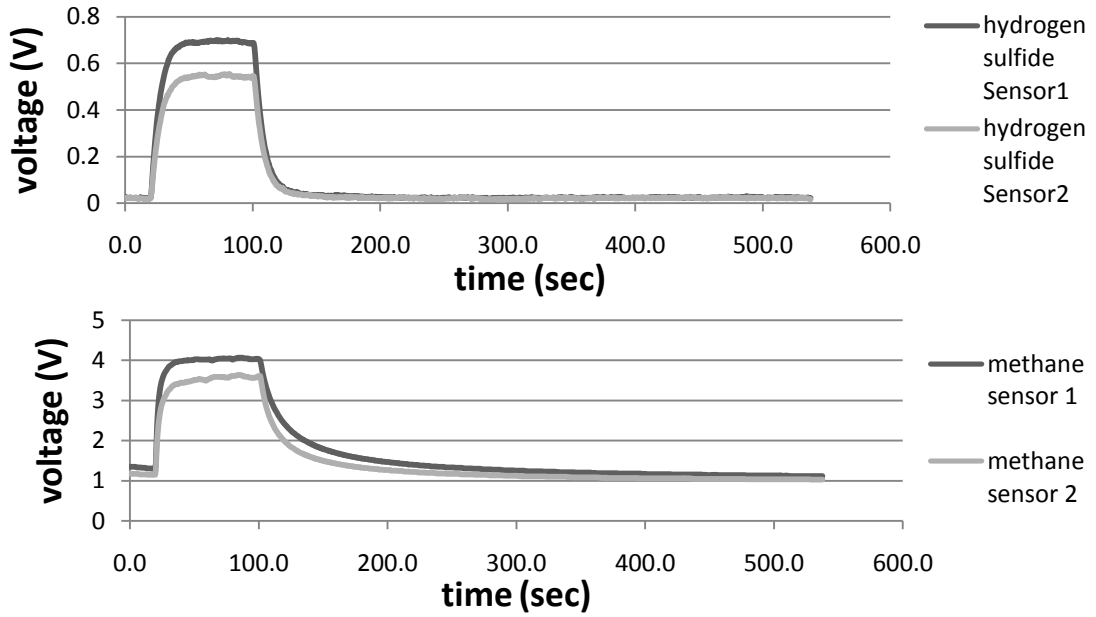


Figure 3.11: The Voltage Signals from the Gas Sensors when a Forty-five Second Pulse of Biogas was added to the Diluted Flow

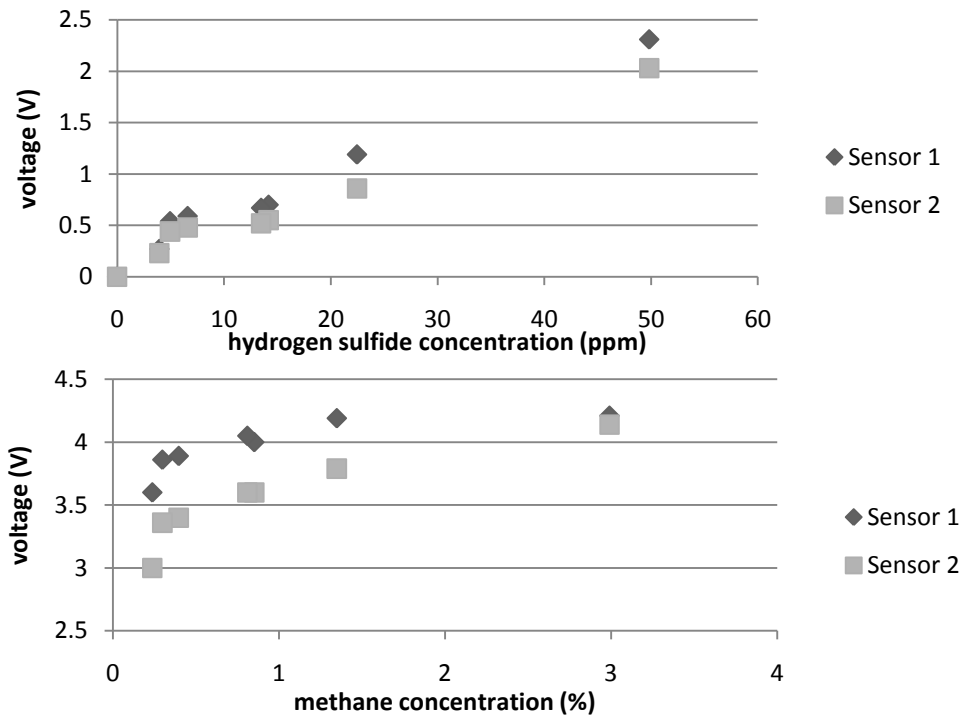


Figure 3.12: The Concentration versus the Flow Sensor Voltages

Using a linear regression for the hydrogen sulfide sensor and a normal regression for the methane sensor it was possible to produce a characteristic equation relating the voltage signals coming from the gas sensors to the concentrations of the component gases. (See figure 3.13)

The hydrogen sulfide sensors were rated between 0 and 100 ppm and the methane sensor was between 0% and 10%. The resolution of the concentration sensors were limited by the resolution of the flow sensors and the 12-bit analog to digital sensor. The gas sensors operated between 0 and 5V and had a resolution of 2.44×10^{-4} V.

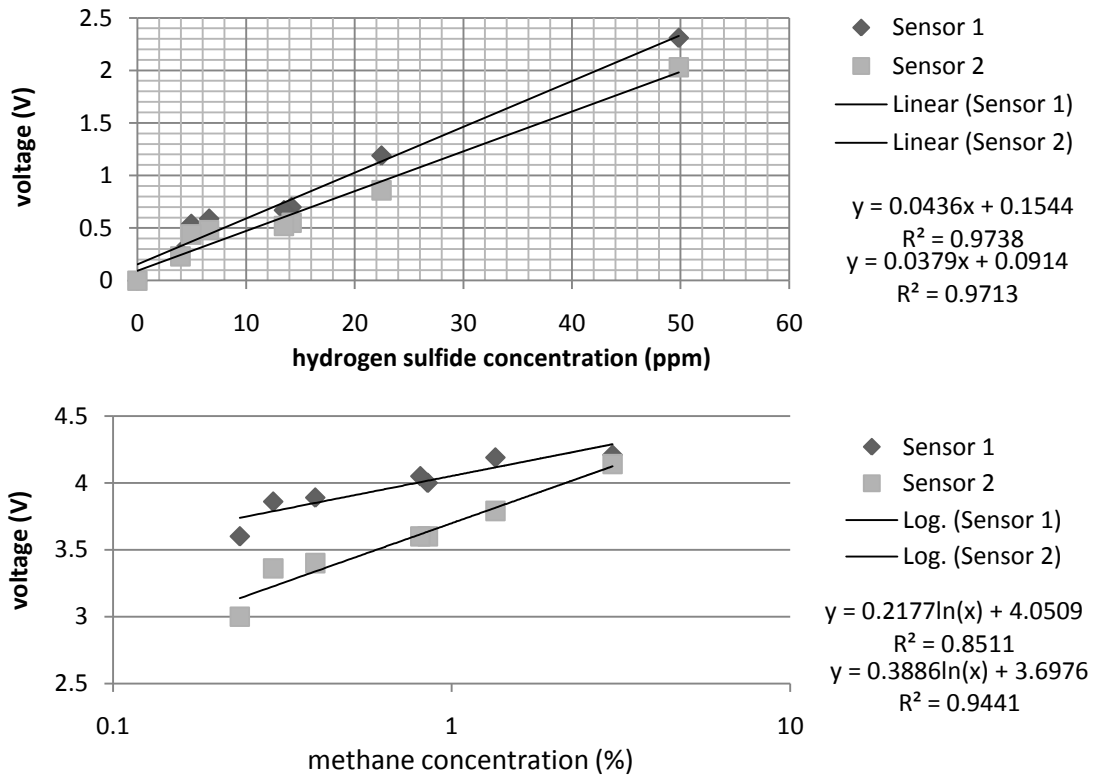


Figure 3.13: The Concentration Regressed on the Flow Sensor Voltage

3.5 Conclusion

A new inexpensive instrument built from off the shelf components was developed to measure both the flow and concentration of methane and hydrogen sulfide in biogas. This system used the properties of a Poiseuille flow to measure the flow of the gas. A maximum velocity was measured and converted into a volumetric flow. This system used the electro-chemical properties of liquid and solid-state solutions to measure the concentration of hydrogen sulfide and methane in the flow.

Using electronic sensors to detect the quality of biogas opens up the possibility of using on-line monitoring and closed loop control of digesters to improve of biogas quality. The limitation of the device is the sensors require oxygen to work. Before biogas can be burned, it must be diluted with oxygen so this system may find a practical niche in that situation. This instrument is best suited for its primary purpose which is to test the effectiveness of systems that remove hydrogen sulfide from biogas.

CHAPTER 4

Testing Biogas Passed Through a Gas-Gas Membrane System for Hydrogen Sulfide Removal

4.1 Introduction

Higher fuel costs are driving research into selective gas-gas membranes. Gas-gas membranes are already being used to improve sour natural gas; so there may be potential for membranes to improve biogas. Biogas quality can be improved by separating biogas and removing the acid gases – of which the most detrimental to biogas quality is hydrogen sulfide (as shown in table 4.1). Most hydrogen sulfide removal technologies require a high energy phase change, a complex mechanism, or a large mechanical footprint which is not required by a gas-gas membrane system. One such gas-gas membrane system was tested for its ability to remove hydrogen sulfide using a new, experimental sensor system developed specifically for testing hydrogen sulfide removal.

Table 4.1: Metrics for Biogas Quality Based on the Hydrogen Sulfide Concentration

Concentration of Hydrogen Sulfide	Usefulness of biogas
4000 ppm	Typical Biogas
600 ppm	High Quality Biogas
below 100 ppm	Safe for Natural Gas lines
below 4 ppm	Can be Sold Commercially

Information from Hao, Rice and Stern (2002)

Selective gas-gas membrane research started in 1866 when Graham reported a rubber polymeric membrane increased the concentration of oxygen in air from 21% to 41%. Based on this work, he proposed the absorption - diffusion - dissolution model for membrane transport (Ghosal and Freeman, 1994), which is similar to the transport model described in this research.

This research is one of the few attempts to study gas-gas membrane technology as a means to remove hydrogen sulfide from animal manure biogas since a 1988 study where twelve membranes were tested. None of the membranes were effective for removing hydrogen sulfide (Kayhanian and Hills, 1988). These membranes were made of only a single material. The technology has since advanced to include composite membranes. Composite membranes use different combinations of materials with various sorption and sieving properties. These materials include: cellulose acetate (Stern et al., 1998), polyimide (Hao, Rice and Stern, 2002; Quinn and Laciak, 1997; Hillock, 2005; Harasimowicz et al., 2007), polypropylene (Kreulen et al., 1992), polysulfone (Stern et al., 1998; Harasimowicz et al., 2007), zeolite (Zhu et al., 2005), and tri-bromodi-phenylopolycarbonate (Harasimowicz et al., 2007).

4.2 Theory

4.2.1 Selectivity Mechanisms

Membranes use two different mechanisms to select one gas over another: diffusivity and sorption.

A diffusivity difference between two gases means the gas with a smaller molecular size passes through a porous structure faster than the gas with large molecular size. The relative size of the molecule can be empirically estimated by measuring critical volume. A list of critical volumes is given in table 4.2. Diffusivity may be affected by the shape of a molecule (see figure 4.1). An asymmetric molecule like hydrogen sulfide can pass rapidly through a membrane by a series of diffusion jumps along its long axis (Faure et al., 2007).

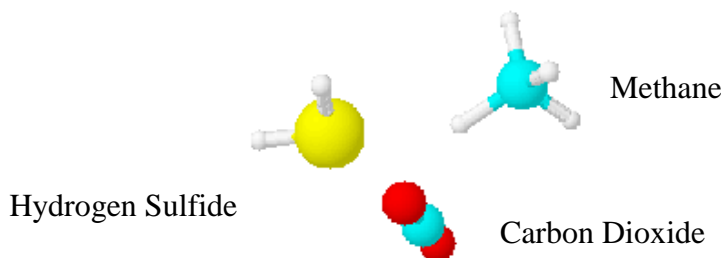


Figure 4.1: The Molecular Shapes of Component Gases in Biogas

A sorption difference between two gases means one gas will dissolve into and form again on the other side of a membrane faster than the other. The ability of a gas to sorb through a membrane is related to critical temperature (the temperature at the triple point). A gas with a lower critical temperature will sorb quickly through a membrane because it can condense on the face of the membrane quickly. The critical temperatures of different gases are given in table 4.2 (Lin and Freeman, 2005).

Table 4.2: Properties of Component Gases used to Select one Gas Over the Other

Penetrant	Critical Volume ($\frac{cm^3}{mole}$)	Critical Temperature ($^{\circ}K$)
H ₂	65.1	33.24
N ₂	89.8	126.20
CH ₄	99.2	191.05
CO ₂	93.9	304.21
H ₂ S	98.5	373.53

Between hydrogen sulfide and methane, there is not as much difference between critical volumes as there is between the critical temperatures. Because of the critical temperature difference it is better to separate biogas using a membrane designed for sorption. Hydrogen sulfide – which is the unwanted gas – sorbs faster than methane through a membrane, therefore a membrane separating biogas by sorption has to be in a

reverse selective configuration. In a reverse selective configuration the hydrogen sulfide is squeezed out of the biogas through the membrane leaving the methane behind in the retentate.

In order to sorb, the gases must dissolve into the surface of the membrane. When acid gases like hydrogen sulfide dissolve into a membrane, the membrane absorbs the gas and swells up. This swelling is referred to as plasticization (Hillock, 2005).

After plasticization, the concentration of a gas on the surface of the membrane can be modeled using Henry's law. (Other isotherms may be used for this step, but Henry's Law is the simplest and the one most commonly used in literature.) Henry's Law is given in equation 4.1. C^{H_2S} is the concentration of hydrogen sulfide at the surface of the membrane, $K_H^{H_2S}$ is Henry's constant for hydrogen sulfide, and p^{H_2S} is the partial pressure of hydrogen sulfide in the biogas.

$$C^{H_2S} = K_H^{H_2S} \cdot p^{H_2S} \quad (4.1)$$

To quantify separation performance (throughput) of the membrane the model includes diffusivity. Diffusion is described by Fick's law which is given in equation 4.2. In this equation J^{H_2S} is diffusion flux of hydrogen sulfide through the membrane, D^{H_2S} is the diffusion coefficient for hydrogen sulfide, x is the length or thickness of the membrane, and $\partial C/\partial x$ is the concentration gradient across the membrane.

$$J^{H_2S} = -D^{H_2S} \left(\frac{\partial C^{H_2S}}{\partial x} \right) \quad (4.2)$$

Integrating diffusion across length of the membrane (equation 4.3) gives the empirical form of the equation. $C_H^{H_2S}$ is the concentration of hydrogen sulfide on the high pressure side of the membrane, while $C_L^{H_2S}$ is the concentration of hydrogen

sulfide on the low pressure side of the membrane. l is the thickness (length) of the membrane.

$$J^{H_2S} = \int_0^l -D^{H_2S} \left(\frac{\partial C^{H_2S}}{\partial x} \right) dx = D^{H_2S} \frac{C_H^{H_2S} - C_L^{H_2S}}{l} \quad (4.3)$$

Putting dissolution and diffusion steps in series yields equation 4.4 where $p_H^{H_2S}$ is the partial pressure of hydrogen sulfide on the high pressure side of the membrane and $p_L^{H_2S}$ is the partial pressure of hydrogen sulfide on the low pressure side of the membrane.

$$J^{H_2S} = D^{H_2S} \cdot K_H^{H_2S} \frac{p_H^{H_2S} - p_L^{H_2S}}{l} \quad (4.4)$$

Permeability is defined as the diffusion coefficient times Henry's constant for a particular gas crossing the membrane. (Barrer, 1927) (See equation 4.5) Permeability is defined with a capital P .

$$P^{H_2S} = D^{H_2S} \cdot K_H^{H_2S} \quad (4.5)$$

Volumetric flow of the gas equals the flux of the gas times the area of the membrane. Equation 4.6 is for volumetric flow across the membrane with A as the area of the membrane.

$$Q^{H_2S} = J^{H_2S} \cdot A = P^{H_2S} \cdot A \frac{p_H^{H_2S} - p_L^{H_2S}}{l} \quad (4.6)$$

Rearranging the terms in equation 4.6 yields permeability in all measurable quantities.

$$P^{H_2S} = \frac{A \cdot (p_H^{H_2S} - p_L^{H_2S})}{Q^{H_2S} \cdot l} \quad (4.7)$$

The unit for permeability is a barrer. Assuming standard temperature and pressure conditions a barrer is defined in equation 4.8.

$$1Barrer = 1 \times 10^{-10} \frac{cm^3 \cdot cm}{cm^2 \cdot sec \cdot cmHg} \quad (4.8)$$

Permeability is generally simplified if the membrane is a asymmetric or composite membrane such as the one in this experiment. The thickness term (l) is dropped from equation 4.7 defining a gas permeation unit (GPU) (see equation 4.9).

$$1GPU = 1 \times 10^{-10} \frac{cm^3}{cm^2 \cdot sec \cdot cmHg} \quad (4.9)$$

If the membrane is working properly, different gases will have different permeabilities. The ratio of permeabilities for two different gases is the membranes selectivity (α). Selectivity is given in equation 4.10).

$$\alpha^{\frac{H_2S}{CH_4}} = \frac{P^{H_2S}}{P^{CH_4}} \quad (4.10)$$

One of the challenges in membrane selection is to get a membrane that has both high permeability (production) for the target gas and high selectivity (efficiency).

4.3 Materials

The membrane in this experiment works by passing acid gas molecules, like

hydrogen sulfide, and retaining methane. It is an asymmetric membrane with the selective layer composed of a polyamide-polyether block copolymer on top of a macro porous layer. Polyamide-polyether copolymers are an ideal material because it remains a rubber at temperatures as low as 0°C and as high as 150°C (Blume and Pinnau, 1990).

Simulated biogas that contained 1000 ppm hydrogen sulfide, 60% methane, balanced with carbon dioxide was supplied from a pressurized tank through a stainless steel regulator into custom made membrane holder that resembled the holder used by Kayhanian and Hills (1988). The membrane holder was made of two 15 x 15 x 0.6 cm (6" x 6" x 1/4") steel plates with two couplings welded into each plate. Small c-clamps clamped the steel plates together at each of the four corners. Two rubber sheets were made into gaskets for the membrane. An exploded view of the holder assembly with the membrane is given in figure 4.2.

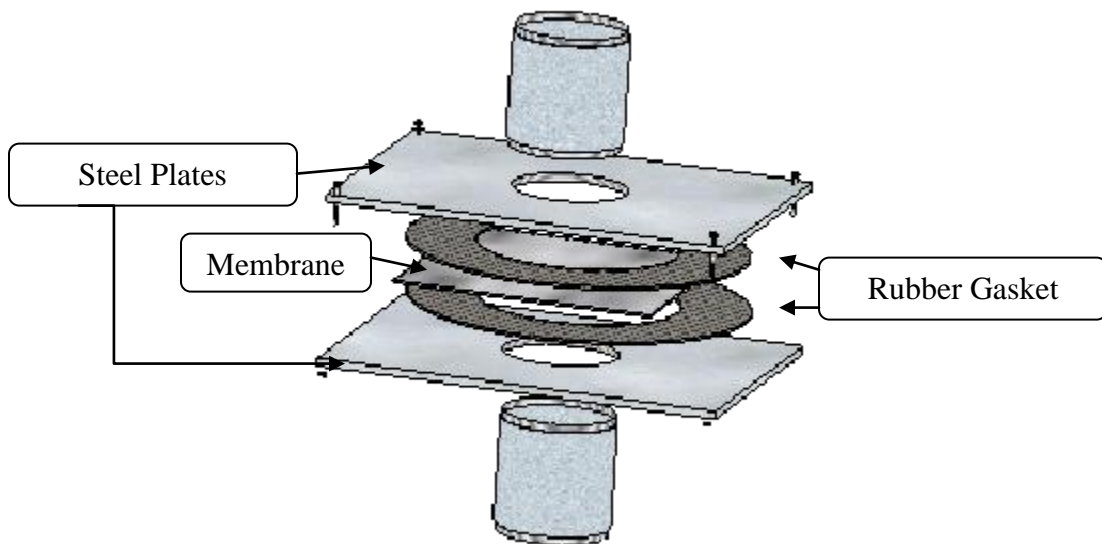


Figure 4.2: An Exploded View of the Membrane Holder with the Membrane in it

The membrane cell, which held the pressurized gas behind the membrane, was fastened to the holder and made from a 2.5 x 2.5 x 2.5 cm (1"x1"x1") T-fitting and a coupling. Rubber stoppers were inserted into pressurized end of the cell and into the

pipe facing the membrane. A polyethylene tube was threaded from the pressurized stopper, through the stopper close to the membrane and back through the stopper close to the membrane. The tube was cut and twisted in a manner that forced the biogas across the membrane. The volume of the space behind the membrane was reduced as much as possible to minimize transient effects caused by air being flushed out when it was pressurized with biogas.

All parts of the membrane cell were made of polyethylene, polytetrafluoroethylene, rubber, stainless steel, or were coated with fiberglass resin to prevent the absorption or accumulation of hydrogen sulfide.

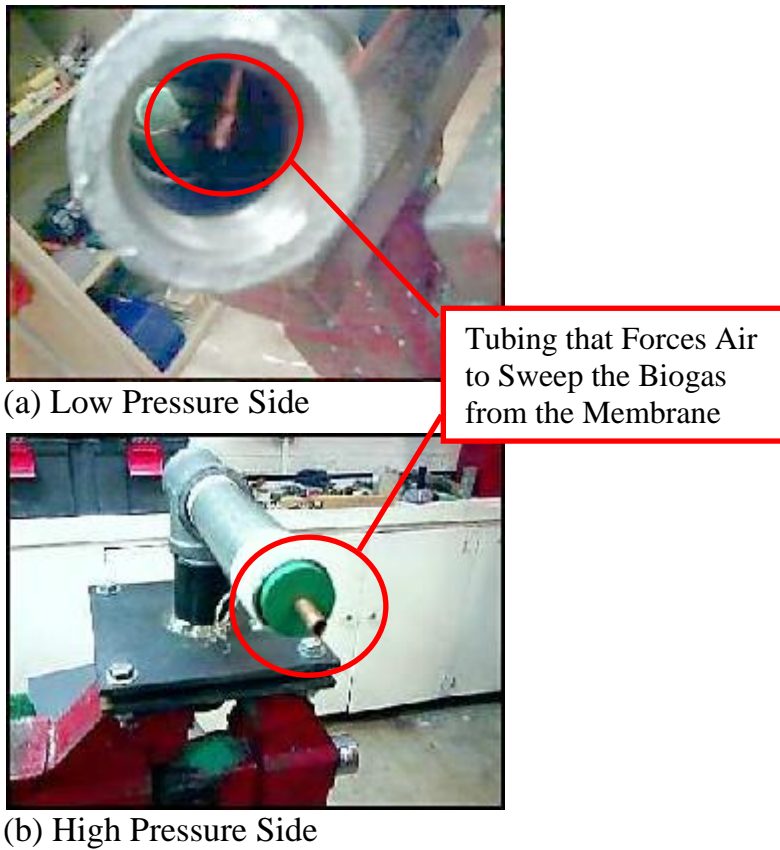


Figure 4.3: Pressurized Chamber Mounted on the Membrane Holder

Two types of chemical sensors and the signal conditioning circuitry described in chapter three were used to detect hydrogen sulfide and methane concentrations. These sensors were mounted, as shown in figure 4.4, in a way that directed the gas stream directly into the sensors.



Figure 4.4: Gas Sensors Mounted on the Apparatus

Figure 4.5 is a close-up of the different mechanisms attached to the membrane holder. On the left side of the figure is the cylinder containing biogas and the regulator. Under the square plates of the holder is the pressurized chamber shown in figure 4.3. On the right of the holder is a pin valve used for restricting the release of biogas from the retentate. The setting of the pin valve is determined by the number of turns from its closed position. Two fiberglass tubes capture and dilute the biogas released from the permeate and the retentate side of the membrane with air. These tubes are long and rigid with smooth walls to promote a laminar velocity profile. Inside each fiberglass tube two pitot tubes are mounted for the purpose of detecting the change in pressure as the gas moved down the tubes. Air is driven through the fiberglass tubes using a blower from a shop vacuum cleaner. The air flow is controlled by adjusting two ball valves on a Y-connector. Cups with the bottom cut out of them are attached to the outlet of the

fiberglass tubes to both hold the gas sensors and deflect wind. Pieces of surveyor's tape are draped over the cups as a safety feature to verify the air was flowing.

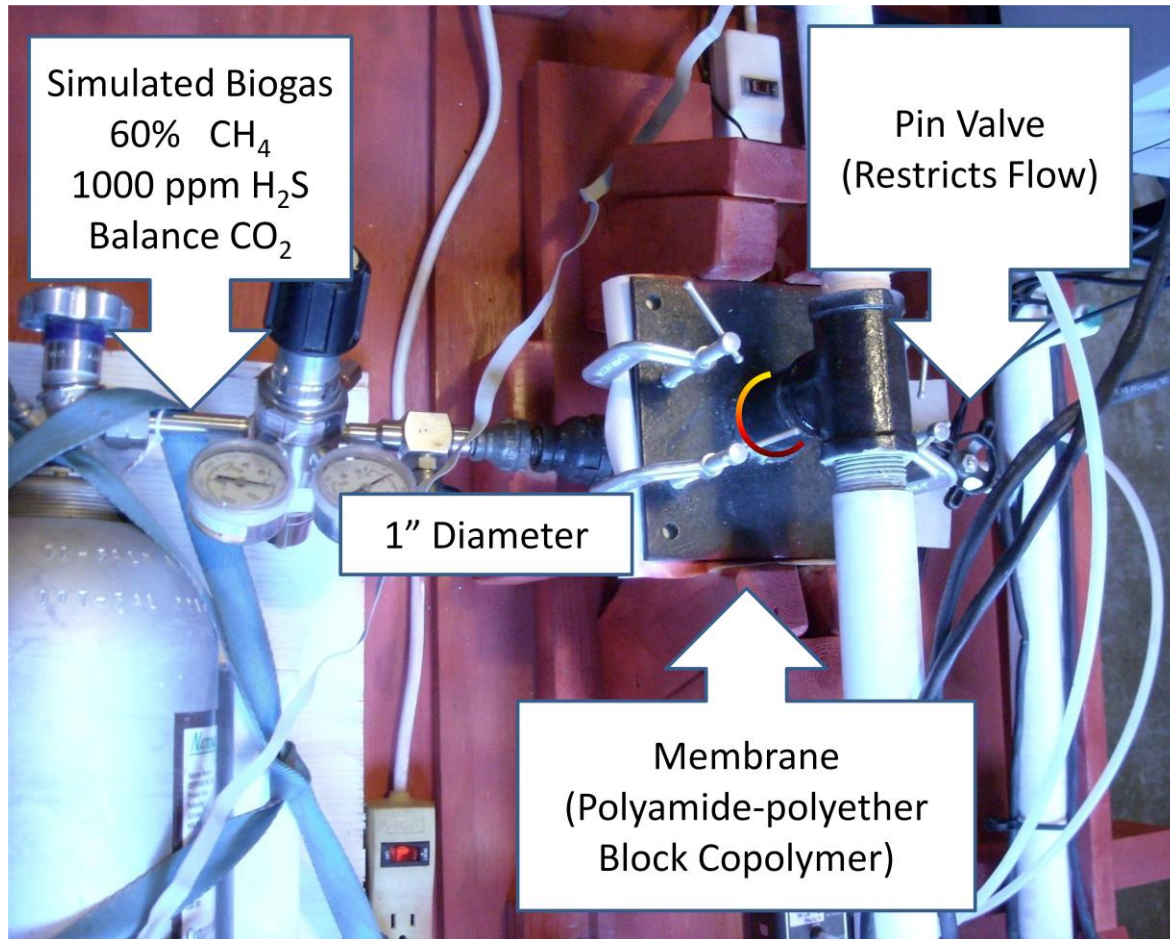


Figure 4.5: Close-up of Mechanisms Attached to Membrane Holder



Figure 4.6: Complete Apparatus

4.4 Methods

There were conflicts between the quality of the results and safety of the experiment. A dilution ratio between forty and one hundred parts air to biogas had to be used to prevent the temperature of the air/biogas mixture's flash point from dropping low enough to explode. Because of the dilution, specialized conditioning circuitry was designed and special data processing methods used for high precision measurement of the volumetric flows.

Because hydrogen sulfide is toxic and the apparatus was too large to fit under a hood, the experiment had to be performed outdoors and attended constantly. Temperature was impossible to control, so thermal drift had to be compensated for in very small voltage signals. This was done by subtracting the linear time dependent trend in the quiescent flow voltage signal observed before the biogas was pressurized from the entire signal including the portion after the biogas was pressurized.

The measurement system for the apparatus was fully automated. When the software driving the apparatus was started, data was continuously recorded. Each gas

concentration measurement was recorded once per second. Each flow measurement was recorded one hundred times a second and then averaged for that second to eliminate noise.

After the voltages were recorded, post processing was done using spreadsheet software. The first filter rejected voltage spikes five standard deviations from the mean over a twenty second sliding window. The final filter was an averaging twenty second sliding window used to smooth out the curves.

When the post processing was complete the voltage values from each of the sensors were converted into a volumetric flows and concentrations using known calibration coefficients.

The correct operation of the apparatus was verified by calculating the input concentration based on the output volumetric flows and concentrations and comparing them to known input concentrations. If the input concentration of the biogas matched the actual concentration of the simulated biogas the system was considered functional. Figure 4.7 is a diagram of all of the different flows and concentrations in this system used for computing the input concentration.

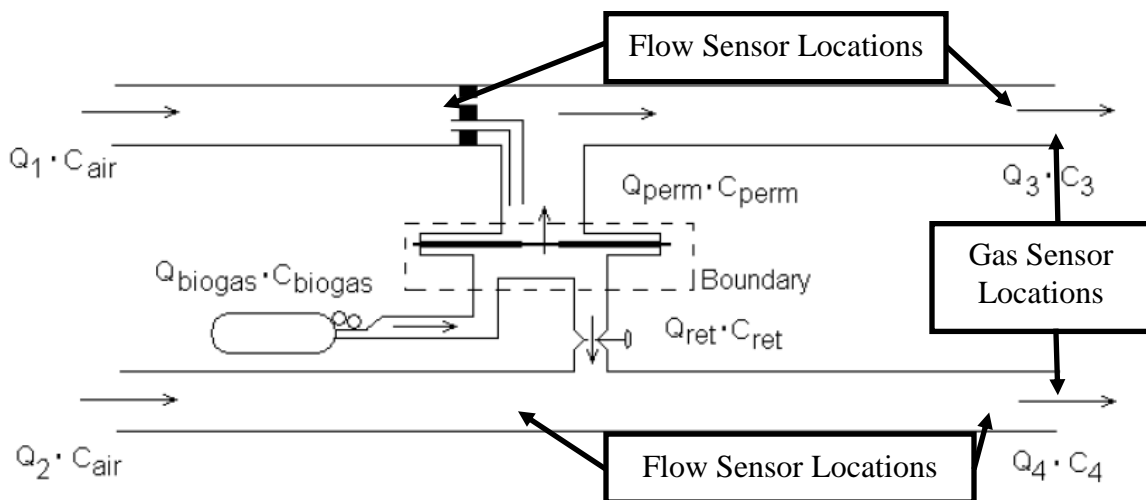


Figure 4.7: Diagram Showing Flows Through the Membrane

The boundary for the mass balance is around both the membrane. One flow comes in and two flows go out. The flow coming in is from the cylinder filled with biogas. The two flows going out go out either through the membrane -- permeate flow - or by it (through the pin valve) -- retentate flow.

Individual gases (such as hydrogen sulfide) in this system are assumed to behave as an ideal gas. The mass of the component gases in the system are proportional (using the atomic number n) to the number of moles. The number of moles (m) in the gas in the system is proportional (k) to concentration (C). From the ideal gas relation the moles of gas present can be related to the pressure (p), volume (V), ideal gas constant (R), and Temperature (T) as shown in equation 4.11.

$$m = C \cdot k \cdot n = \frac{C \cdot k \cdot p \cdot V}{R \cdot T} \quad (4.11)$$

When the simulated biogas first encounters the membrane, the membrane absorbs the acid gases. When the membrane has been exposed for 2.6 minutes to the biogas, it swells, or plasticizes. After the membrane saturates, there is no accumulation.

Because all gases are assumed ideal and because there is no accumulation, equation 4.12 can be written to show that the number of moles (N) of gas that enter the system at any given moment of time (t) leave the system through either the permeate ($perm$) stream or the retentate (ret) stream.

$$\frac{dN_{in}}{dt} = \frac{dN_{perm}}{dt} + \frac{dN_{ret}}{dt} \quad (4.12)$$

Using equation 4.12 for bulk flow and setting the concentration terms to unity in equation 4.11 equation 4.13 can be derived. This equation reduces to 4.14 to show that there is a balance between the flow in and the flow out.

$$\frac{k \cdot p_{in}}{R \cdot T} \cdot \frac{dV_{in}}{dt} = \frac{k \cdot p_{out}}{R \cdot T} \cdot \frac{dV_{perm}}{dt} + \frac{k \cdot p_{out}}{R \cdot T} \cdot \frac{dV_{ret}}{dt} \quad (4.13)$$

$$\frac{dV_{in}}{dt} = \frac{p_{out}}{p_{in}} \left(\frac{dV_{perm}}{dt} + \frac{dV_{ret}}{dt} \right) \quad (4.14)$$

The instantaneous change in volume terms can be converted into flow terms.
(see equation 4.15)

$$Q_{in} = \frac{p_{out}}{p_{in}} (Q_{perm} + Q_{ret}) \quad (4.15)$$

Equation 4.16 is the general form of the mass balance.

$$\text{mass accumulated} = \text{mass flowing in} - \text{mass flowing out} + \text{mass generated} \quad (4.16)$$

As mentioned earlier, there is no accumulation or mass generation in the system. This systems mass balance can be reduced to equation 4.17.

$$\text{mass flowing in} = \text{mass flowing out} \quad (4.17)$$

Flow in and flow out can be derived by plugging in values based on the ideal gas assumption. (See equations 4.18 and 4.19)

$$\text{mass flowing in} = \frac{dm_{in}}{dt} = C_{in} \cdot k \cdot \frac{dn_{in}}{dt} = \frac{k \cdot C_{in} \cdot p_{in}}{R \cdot T} \cdot \frac{dV_{in}}{dt} \quad (4.18)$$

$$\begin{aligned} \text{mass flow out} &= \frac{dm_{perm}}{dt} + \frac{dm_{ret}}{dt} = C_{ret} \cdot k \cdot \frac{dn_{ret}}{dt} + C_{perm} \cdot k \cdot \frac{dn_{perm}}{dt} \\ &= \frac{C_{ret} \cdot k \cdot p_{out}}{R \cdot T} \cdot \frac{dV_{ret}}{dt} + \frac{C_{perm} \cdot k \cdot p_{out}}{R \cdot T} \cdot \frac{dV_{perm}}{dt} \end{aligned} \quad (4.19)$$

Plugging 4.18 and 4.19 into each other yields equation 4.20 which is used to verify the balance of the system.

$$\frac{k \cdot C_{in} \cdot p_{in}}{R \cdot T} \cdot \frac{dV_{in}}{dt} = \frac{C_{ret} \cdot k \cdot p_{out}}{R \cdot T} \cdot \frac{dV_{ret}}{dt} + \frac{C_{perm} \cdot k \cdot p_{out}}{R \cdot T} \cdot \frac{dV_{perm}}{dt} \quad (4.20)$$

Variables k, R and T cancel out in equation 4.20 and yields equation 4.21.

$$p_{in} \cdot C_{in} \cdot \frac{dV_{in}}{dt} = p_{out} \left(C_{ret} \cdot \frac{dV_{ret}}{dt} + C_{perm} \cdot \frac{dV_{perm}}{dt} \right) \quad (4.21)$$

Substituting flow for instantaneous change in volume yields equation 4.22.

$$p_{in} \cdot C_{in} \cdot Q_{in} = p_{out} (C_{ret} \cdot Q_{ret} + C_{perm} \cdot Q_{perm}) \quad (4.22)$$

Substituting equation 4.16 into 4.22 yields the equation 4.23 which can be reduced to equation 4.24. Equation 4.24 is used to calculate the input concentrations that validate the operation of this device.

$$p_{in} \cdot C_{in} \cdot \frac{p_{out}}{p_{in}} (Q_{perm} + Q_{ret}) = p_{out} (C_{ret} \cdot Q_{ret} + C_{perm} \cdot Q_{perm}) \quad (4.23)$$

$$C_{in} \cdot (Q_{perm} + Q_{ret}) = (C_{ret} \cdot Q_{ret} + C_{perm} \cdot Q_{perm}) \quad (4.24)$$

A different mass balance around the dilution tubes can be used for the determination of Q_{ret} , C_{ret} , Q_{perm} , and C_{perm} . These flows in – as shown in figure 4.7 – are diluted by atmospheric air (Q_1 and Q_2) which has no methane or hydrogen sulfide. The hydrogen sulfide and methane that leave these tubes is the same that enters these tubes from the two biogas flows, hence equations 4.25 and 4.26.

$$Q_{perm} \cdot C_{perm} = Q_3 \cdot C_3 \quad (4.25)$$

$$Q_{ret} \cdot C_{ret} = Q_4 \cdot C_4 \quad (4.26)$$

Q_3 , C_3 , Q_4 , and C_4 are all quantities measurable by the sensors on the apparatus. Q_{perm} and Q_{ret} is equal to the difference between the measured volumetric flow at time t_0 when no biogas is flowing and the flow at time t_1 when the system pressurized and the biogas has reached equilibrium. This shift in equilibrium is expressed in equations 4.27 and 4.28, which are used to calculate Q_{perm} and Q_{ret} .

$$Q_{perm} = Q_3(t_1) - Q_3(t_0) \quad (4.27)$$

$$Q_{ret} = Q_4(t_1) - Q_4(t_0) \quad (4.28)$$

A variation of equations 4.27 and 4.28 can be combined with compensation for the thermal drift. At time t_0 there is a time dependent slope in the flow signal caused by a temperature change of the flow sensors. The flow signal can be corrected at time t_1 by

subtracting the time dependent part as well as the time independent part of the flow signal. As shown in figure 4.8 the determination of equations 4.27 and 4.28 and the removal of thermal drift can be accomplished in a single step by subtracting the linear drift from the raw voltage signal from the sensor before it is converted into a volumetric flow.

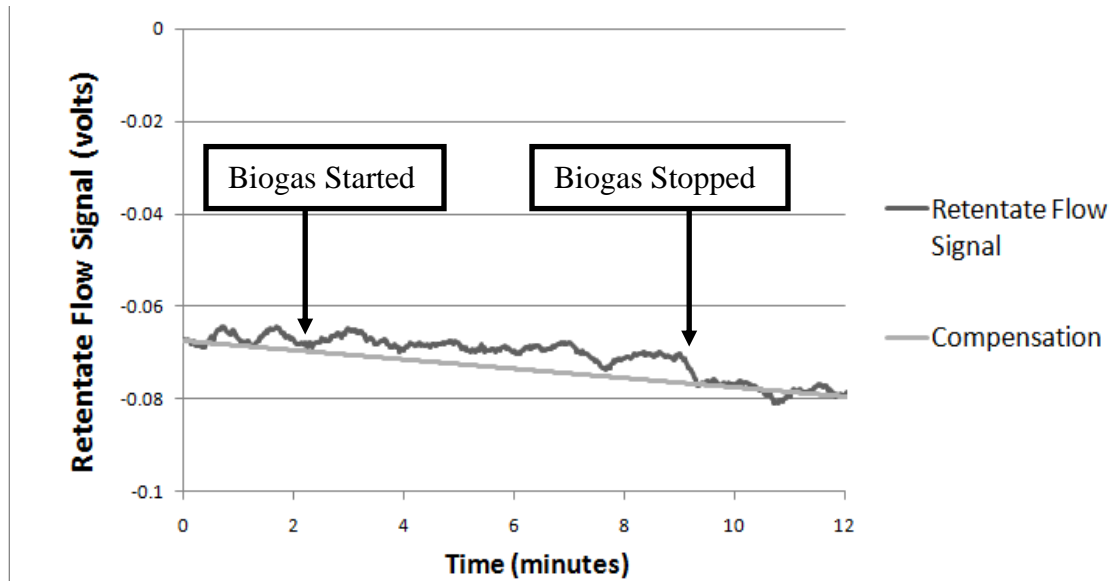


Figure 4.8: Thermal Correction Curve Superimposed on the Raw Voltage Curve from Flow Sensor

4.5 Data/Results

The membrane was tested at a pressure of 2 PSI, which is a low pressure ideal for an anaerobic digester. Hydrogen sulfide was observed on the retentate side of the membrane 2.6 minutes before being observed on the permeate side when the system was first pressurized (while the membrane was saturating).

The input concentrations calculated from the sensor readings obtained using the method in chapter 3. The equations used were 4.24, 4.25, and 4.26 and the results are

shown in figure 4.9. The input concentration values are close to the known input concentrations of 1000 ppm hydrogen sulfide and 60% methane.

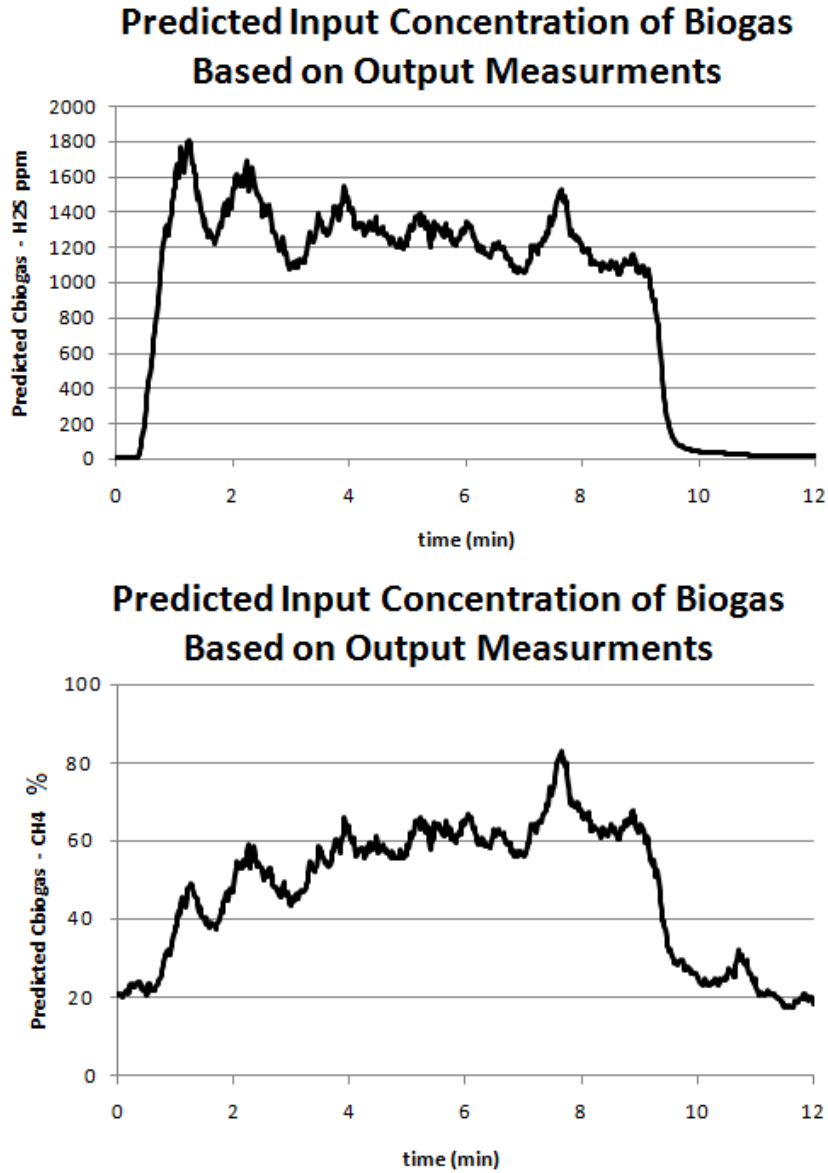


Figure 4.9: Calculation of the Input Concentrations Based on the Output Concentrations over Time

Using equations 4.24 through 4.28 a mass balance was solved for. The results of all of the variables are given in table 4.3.

Table 4.3: Results of Final Mass Balance

Variable	Value	Units	Standard Deviation
Measured Values			
$Q_1(0)$	8600	cm ³ /sec	68
$Q_2(0)$	51,000	cm ³ /sec	230
* $Q_3 - Q_1$	96	cm ³ /sec	14
* $Q_4 - Q_2$	990	cm ³ /sec	137
* $C_{H_2S,3}$	0.48	ppm	0.13
* $C_{H_2S,4}$	23	ppm	8.6
* $C_{CH_4,3}$	0.0036	%	0.00018
* $C_{CH_4,4}$	0.012	%	0.0032
Calculated Values			
$C_{H_2S,perm}$	43	ppm	
$C_{H_2S,ret}$	1184	ppm	
$C_{CH_4,perm}$	32	%	
$C_{CH_4,ret}$	62	%	
Calculated Values for Comparison			
$Q_{H_2S,in}$	1.08	cm ³ /sec	
$Q_{H_2S,out}$	1.18	cm ³ /sec	
$Q_{CH_4,in}$	650	cm ³ /sec	
$Q_{CH_4,out}$	640	cm ³ /sec	
$C_{H_2S,in}$	1070	ppm	
$C_{CH_4,in}$	58	%	
Known Values			
$C_{H_2S,in}$	1000	ppm	
$C_{CH_4,in}$	60	%	

*Averaged over 6 minutes, $\Delta P = 2$ PSI, $A = 5.1$ cm²

The measurements for flow, particularly the flow leaving the membrane, were in doubt. The signal for the volumetric flow leaving the membrane was $96 \text{ cm}^3/\text{sec}$ with a standard deviation close to the signal at $14 \text{ cm}^3/\text{sec}$. These signals may be too much in doubt to draw any firm conclusions as of yet based on this data.

In this device the flow had to be diverted into the holder to prevent biogas from collecting behind the membrane. This diversion interfered with the pressure measurement. Reducing the amount of diversion necessary should improve the flow signal and open up the possibility of using the pressure measurement to directly calculate volumetric flow. The way to make this change in a future version of this device would be to bring the tubes as close as possible to the membrane.

Another improvement to this device would be to include a set of null pressure sensors. These null pressure sensors should be capped so no flow is measured. The voltage signal from the pressure sensors would be subtracted from the voltage signal on the null sensors. This would correct for thermal drift and would possibly eliminate some common mode noise that would create an even better flow signal.

4.6 Conclusion

A mass balance was completed around a reverse selective membrane system with the calculated difference between flows based on known input and measured output concentrations coming within 15% of each other. Though the volumetric flow measurements were in doubt, this device was able to determine that using a 20 cm^2 polyamide membrane under low pressures suitable for a digester (2 PSI) will increase methane concentration in biogas from 60% to 62% but is not effective at removing hydrogen sulfide. The membrane requires more pressure than what is acceptable in an anaerobic digester. A blower or compressor may be required to use a membrane.

Measurements in this experiment could be improved by using a set of null

pressure and gas sensors located near the other sensors, but not exposed to the gas flows, to generate a quiescent signal for subtracting out thermal drift and common mode noise. This experiment could further be improved by planning for a smooth flow around the membrane.

This research is by no means complete, but it is a start into the possibility of a small and simple membrane to improve the quality of biogas and a monitoring system to verify the membrane is working properly.

BIBLIOGRAPHY

- Angenent, L., K. Karim, M. Al-Dahhan, B. Wrenn and R. Domiguez-Espinosa. 2004. Production of bioenergy and biochemicals from industrial and agricultural wastewater. *Trends in Biotechnology* 22(9):477–485.
- Arogo, J., R. Zhang, G. Riskowski and D. Day. 2000. Hydrogen sulfide production from stored liquid swine manure: a laboratory study. *Transactions of the ASAE* 43(5):1241–1245.
- Barrer, R. 1927. Permeation, diffusion and solution of gases in organic polymers. *J. Am. Chem. Soc* 49:427.
- Blume, I. and I. Pinnau. 1990. Composite membrane, method of preparation and use. US Patent 4,963,165.
- Bothi, K. 2007. Characterization of biogas from anaerobically digested dairy waste for energy use. Master's thesis Cornell University.
- Brown, B. 2004. H₂S multiphase flow loop CO₂ corrosion in the presence of trace amounts of hydrogen sulfide. Master's thesis Ohio University.
- Cantrell, K., K. Ro, D. Mahajan, M. Anjom and P Hunt. 2007. Role of thermochemical conversion in livestock waste-to-energy treatments: obstacles and opportunities. *Industrial & Engineering Chemistry Research* 46(26):8918–8927.
- Cappenberg, T.E. 1975. A study of mixed continuous cultures of sulfate-reducing and methane-producing bacteria. *Microbial Ecology* 2(1):60–72.
- Chang, F.H. 2004. Energy and sustainability comparisons of anaerobic digestion and thermal technologies for processing animal waste. *ASAE/CSAE meeting, paper 44025*.
- Chen, Y., J. Cheng, K. Creamer. 2008. Inhibition of anaerobic digestion process: a review. *Bioresource Technology* 99(10):4044-4064
- Choinière, Y. 2004. Explosion of a deep pit finishing pig barn, investigation report on biogas production. Ottawa, Ontario, Canada: ASAE/CSAE Meeting.
- Cypionka, H. 1986. Sulfide-controlled continuous culture of sulfate-reducing bacteria. *Journal of Microbiological Methods* 5(1):1–9.

- D. Chynoweth, A. Wilkie and J. Owens. 1998. Anaerobic processing of piggery wastes: a review. Orlando Florida: ASAE Annual International Meeting.
- Faure, F., B. Rousseau, V. Lachet and P. Ungerer. 2007. Molecular simulation of the solubility and diffusion of carbon dioxide and hydrogen sulfide in polyethylene melts. *Fluid Phase Equilibria* 261(1-2):168–175.
- Garrison, M. and T. Richard. 2005. Methane and manure: feasibility analysis of price and policy alternatives. *Transactions of the ASAE* 48(3):1287–1294.
- Ghosal, K. and B. Freeman. 1994. Gas separation using polymer membranes: an overview. *Polymers for Advanced Technologies* 5(11):673–697.
- Goode, P. 1989. Wear mechanisms in ferrous alloys. *Nuclear Instruments and Methods in Physics Research Section B* 39(1-4):521–530.
- Goodrich, P. and D. Schmidt. 2002. Anaerobic digestion for energy and pollution control. Number 024188 Chicago, Illinois: ASAE.
- Gordon, R., M. Bertram and T. Graedel. 2006. Metal stocks and sustainability. *Proceedings of the National Academy of Sciences* 103(5):1209–1214.
- Hamilton, W. 1985. Sulphate-reducing bacteria and anaerobic corrosion. *Annual Review of Microbiology* 39(1):195–217.
- Hansen, K., I. Angelidaki and B. Ahring. 1999. Improving thermophilic anaerobic digestion of swine manure. *Water Research* 33(8):1805–1810.
- Hao, J., P Rice and S. Stern. 2002. Upgrading low-quality natural gas with H₂S - and CO₂ -selective polymer membranes-part I. process design and economics of membrane stages without recycle streams. *Journal of Membrane Science* 209(1):177–206.
- Harasimowicz, M., P. Orluk, G. Zakrzewska-Trznadel and A Chmielewski. 2007. Application of polyimide membranes for biogas purification and enrichment. *Journal of Hazardous Materials* 144(3):698–702.
- Hickling, A. 1942. Studies in electrode polarisation. Part IV. The automatic control of the potential of a working electrode. *Transactions of the Faraday Society* 38:27–33.
- Hillock, A. 2005. Crosslinkable polyimide mixed matrix membranes for natural gas purification. PhD thesis Georgia Tech.

- Hulshoff Pol, L., P. Lens, A. Stams and G. Lettinga. 1998. Anaerobic treatment of sulphate rich wastewaters. *Biodegradation* 9(3):213–224.
- Iannotti, E., J. Fischer and D. Sievers. 1982. Characterization of bacteria from a swine manure digester. *Applied and Environmental Microbiology* 43(1):136–143.
- Ihokura, K. and J. Watson. 1994. *The Stannic Oxide Gas Sensor: Principles and Applications*. CRC Press Inc.
- Jiang, C., T. Liu and J. Zhong. 1989. A study on compressed biogas and its application to the compression ignition dual-fuel engine. *Biomass* 20(1):53–59.
- Kayhanian, M. and D. Hills. 1988. Membrane purification of anaerobic digester gas. *Biol. wastes* 23(1):1–15.
- KiHyun, K., Y. Choi, E. Jeon and S. Young. 2005. Characterization of malodorous sulfur compounds in landfill gas. *Atmospheric Environment* 39(6):1103–1112.
- Kotelnikova, S. 2002. Microbial production and oxidation of methane in deep subsurface. *Earth-Science Reviews* 58(3):367–395.
- Kreulen, H., G. Versteeg, Smolders C. and Van Swaaij. 1992. Selective removal of H₂S from sour gas with microporous membranes. I: application in a gas-liquid system. *Journal of membrane science* 73(2-3):293–304.
- Lens, P., A. Visser, A. Janssen, L. Pol and G. Lettinga. 1998. Biotechnological treatment of sulfate-rich wastewaters. *Critical Reviews in Environmental Science and Technology* 28(1):41–88.
- Li, N. 1984. Biogas in China. *Trends in Biotechnology* 2(3):77–79.
- Lin, H. and B.D. Freeman. 2005. Materials selection guidelines for membranes that remove CO₂ from gas mixtures. *Journal of molecular structure* 739(1-3):57–74.
- López, D., T. Pérez and S. Simison. 2003. The influence of microstructure and chemical composition of carbon and low alloy steels in CO₂ corrosion. a state-of-the-art appraisal. *Materials and Design* 24(8):561–575.
- Lusk, P. 1998. Methane recovery from animal manures the current opportunities casebook. Technical report NREL/SR-580-25145; ON: DE00009526, National Renewable Energy Lab.,.

McFarland, M. and W. Jewell. 1989. In situ control of sulfide emissions during the thermophilic (55 degree C) anaerobic digestion process. *Water Research* 23(12):1571–1577.

M.Gaidi, B. Chenevier and M. Labeau. 2000. Electrical properties evolution under reducing gaseous mixtures (H₂, H₂S, CO) of SnO₂ thin films doped with Pd/Pt aggregates and used as polluting gas sensors. *Sensors & Actuators: B. Chemical* 62(1):43–48.

Moseley, P. 1997. Solid state gas sensors. *Meas. Sci. Technol* 8:223–237.

NCDACS. 2004. Farm income: Cash receipts from farming by commodity. Accessed Dec. 1, 2005. **URL:** <http://www.agr.state.nc.us/>

Ni, J., A. Heber, D. Kelly and A. Sutton. 2001. Mechanism of gas release from liquid swine wastes. *ASAE Annual International Meeting* .

Nicolai, R. and K. Janni. 1997. Development of a low cost biofilter for swine production facilities. *ASAE Paper* 974040.

Oremland, R. and S. Polcin. 1982. Methanogenesis and sulfate reduction: competitive and noncompetitive substrates in estuarine sediments. *Applied and Environmental Microbiology* 44(6):1270.

Osbern, L.N. and R.O. Crapo. 1981. Dung lung: a report of toxic exposure to liquid manure. *Ann Intern Med* 95(3):312–4.

Pagilla, K. , H. Kim and T. Cheunbarn. 2000. Aerobic thermophilic and anaerobic mesophilic treatment of swine waste. *Water Research* 34(10):2747–2753.

Pesta, Gunther. 2006. Anaerobic digestion of organic residues and wastes -- *Utilization of By-Products and Treatment of Waste in the Food Industry*. Springer. 53-72.

Picken, D. and H. Hassaan. 1983. A method for estimating overhaul life of internal combustion engines including, engines operating on biogas and methane. *J. agric. Eng. Res.* 28:139–147.

Pourbaix, M. 1966. *Atlas of Electrochemical Equilibrium Diagrams in Aqueous Solutions*. Pergamon Press, Oxford.

Quinn, R. and D. Laciak. 1997. Polyelectrolyte membranes for acid gas separations. *Journal of Membrane Science* 131(1):49–60.

Ravanel, S., B. Gakiere, D. Job and R. Douce. 1998. The specific features of methionine biosynthesis and metabolism in plants. *Proceedings of the National Academy of Sciences of the United States of America* 95(13):7805–7812.

Schönheit, P., J. Kristjansson and R. Thauer. 1982. Kinetic mechanism for the ability of sulfate reducers to out-compete methanogens for acetate. *Archives of Microbiology* 132(3):285–288.

Shin, H., J. Park, K. Park and H. Song. 2002. Removal characteristics of trace compounds of landfill gas by activated carbon adsorption. *Environmental Pollution* 119(2):227–236.

Smith, S. 1993. A proposed mechanism for corrosion in slightly sour oil and gas production. *12th International Corrosion Congress* (385).

Stern, S., B. Krishnakumar, S. Charati, W. Amato, A. Friedman and D. Fuess. 1998. Performance of a bench-scale membrane pilot plant for the upgrading of biogas in a wastewater treatment plant. *Journal of Membrane Science* 151(1):63–74.

Stowell, R. and C. Henry. 2003. The economic impacts of various public-policy scenarios for methane recovery on dairy farms. Number 034013 Las Vegas, Nevada: ASAE.

Sudarshan, T. and S. Bhaduri. 1983. Wear in cylinder liners. *Wear* 91(3):269–279.

T., Watson J., Ihokura K. and Colest G. 1993. The tin dioxide gas sensor. *Meas. Sci. Technol* 4:711–719.

Tchobanoglous, G., F. Burton and H. Stensel. 2002. *Wastewater Engineering: Treatment and Reuse*. McGraw-Hill Publishing Co.

Wiser, R. and M. Bolinger. 2007. Can deployment of renewable energy put downward pressure on natural gas prices? *Energy Policy* 35(1):295–306.

Zhu, J., G. Riskowski and M. Torremorell. 1999. Volatile fatty acids as odor indicators in swine manure—a critical review. *Trans. ASAE* 42(1):175–182.

Zhu, W., L. Gora, A. van den Berg, F. Kapteijn, J. Jansen and J. Moulijn. 2005. Water vapour separation from permanent gases by a zeolite-4A membrane. *Journal of Membrane Science* 253(1-2):57–66.

APPENDICIES

APPENDIX A

History of Biogas

During the early 1600's, Jan Baptist van Helmont discovered that fermenting organic matter produced a flammable gas. Alessandro Volta discovered this gas was comprised of mostly methane; and he correlated the amount of methane produced to the amount of organic matter fermented. In the late 1800's Gayon, one of Pasteur's students, discovered animal manure fermented best at 35°C (95°F). As the field of microbiology developed researchers identified both the anaerobic bacteria involved and the best conditions for producing methane by fermentation (Lusk, 1998).

There is evidence to suggest that biogas was being utilized to heat bath water as early as 1000 BC by the Assyrians and later by the Persians. One of the earliest digestion plants was built at in Bombay, India in 1859. In 1895 biogas from sewage was used to fuel street lamps in Exeter, England (Lusk, 1998).

Anaerobic digesters became common during the energy crisis brought on by World War II. Since then the technology has continued to grow worldwide (Lusk, 1998). The technology has been difficult to adapt in the United States because it was developed for small farms and households as opposed to larger farms.

In the United States one of the earliest anaerobic systems for handling swine waste was built in 1972 in Mt. Pleasant, Iowa. It was constructed because of the need to control odors that were drifting into a nearby town (Lusk, 1998). Following the construction of this digester anaerobic digestion technologies like two stage digestion, plug flow reactors, and codigestion were further developed in the United States.

APPENDIX B

Biogas Safety

Extreme caution is urged when working with biogas. Risks when dealing with biogas include explosion, asphyxiation, or hydrogen sulfide poisoning. When dealing with raw manure, infection is a concern (Osbern and Crapo, 1981).

B.1 Explosion

Biogas diluted between 10% and 30% with air is an explosion hazard. In 2003 several explosions on Canadian swine farms were thought to have been caused by biogas exploding (Choinière, 2004).

B.2 Asphyxiation

Asphyxiation from biogas is a concern in an enclosed space where manure is stored. Osbern and Crapo (1981) report one case of a farmer, his son, and a sheriff who died from asphyxiation created by swine manure gas in an enclosed space.

B.3 Hydrogen Sulfide Poisoning

Table B.1 shows the possible health effects due to hydrogen sulfide poisoning.

Table B.1: Health Effects of Hydrogen Sulfide Exposure

Parts per million (ppm)	Possible Health Effects
0.01-0.3	Odor is detectable
	Moderate to strong odor
	Nausea
	Tears
	Headaches
1-10	Sleep loss
	irritation of the eyes
10-150	irritation of the lungs
	severe health effects
150-750	death becomes more likely
>750	death may occur in minutes

B.4 Infection from Swine Wastes

Salmonellosis, Q fever, Newcastle disease, histoplasmosis, cryptosporidiosis, and gardiasis may be transmitted by swine waste (D. P. Chynoweth and Owens, 1998).

APPENDIX C

Extended Explanation for Diagrams

C.1 The Derivation of the Potential - pH Diagram

For the diagram given in figure 2.5 the stability region for condensation droplet in an ideal biogas - iron system is located around points 1, 2, 3, and 4. Each point in the diagram represents a solution with E_0 on the y-axis representing the electrical potential between an uninsulated iron electrode and a standard hydrogen electrode and the x-axis represents the pH of the solution. Hydrogen sulfide primarily affects the pH so points 1 and 2 are labeled to show a system with no hydrogen sulfide and points 3 and 4 show a system with 1000 ppm hydrogen sulfide. The amount of oxygen available in the system primarily affects the potential. Points 1 and 4 are in an anoxic environment and points 2 and three are in a oxygen saturated environment.

The values for these points are derived from the Nernst equation given in C.2. E_0^0 is the standard equilibrium potential in volts. n is the number of electrons transferred in the half reaction. μ^0 is the Gibbs free energy of formation in joules per mole. M is the concentration of a species in the reaction in moles. v is the number of moles involved in the half reaction with a positive sign indicating a product and negative for a reactant. The reaction is the same as equation 2.2.1 using iron as the metal. The derivation for the rest of this diagram is adapted from the derivation in Pourbaix's *Atlas of Electrochemical Equilibria in Aqueous Solutions*(1966).

$$E_0 = E_0^0 + \frac{0.0591}{n} \sum v \log(M) \quad (C.1)$$

$$E_0^0 = \frac{\sum v \mu^0}{23060 n} \quad (C.2)$$

The dotted black lines in the graph show the stability region of water. Between these lines water is stable in its liquid form. Above the lines oxygen gas is more stable than water. Below these lines hydrogen gas is more stable. The solid black lines are the equilibrium lines for iron oxidation given Pourbaix conditions. Pourbaix conditions are the same as standard conditions except the concentration of any dissolved substances other than hydrogen and oxygen derivatives are arbitrarily selected to be 10^{-6} M. The solid red lines are equilibrium lines for the various forms of iron sulfide given Pourbaix conditions. The kinetics of iron corrosion was determined empirically and is given by the green lines in the diagram. The kinetics considered are rapid degradation (> 1 mm/year) and slow degradation (< 0.3 mm/year.) (Pourbaix, 1966)

C.2 The Volumetric Flow Signal Conditioning Circuit

A very specialized circuit had to be built to handle the pressure measurement with the features listed in table 3.1. The flow measurement needed accuracy in the millivolt range so the circuit had to be completely isolated and all electrical noise had to be attenuated. A high quality switching power supply was used to regulate the voltage. This power supply was separated from the computer power supply to attenuate electrical noise that came from the millions of transistor state changes in the processor core that occur during software execution. The sensors were further isolated by using a reference point supplied by the software through a D-A converter instead of a ground reference. This prevented the reference voltage from deflecting when a stray current passed from other parts of the circuit through the non-ideal resistance in the wire grounding the circuit. (This voltage deflection phenomenon is called a floating ground and is often heard as a buzz in a low quality speaker system.) The sensor signal was further protected from noise by using a shielded, twisted pair, 22 gage, solid copper wire that transported the electrical signal from the sensor to the processor board. This prevented cross talk, em noise, and wire resistance from affecting the circuit. To eliminate any noise left over, 100 samples were taken and averaged over ten milliseconds to filter out

high frequency noise. The noise output from this circuit is shown in figure 3.6 similar to the way it would appear in an oscilloscope. The normally 20 mV thermal noise was in the circuit was attenuated to less than 1 mV.

APPENDIX D

Software

```
/*
Membrane_Filtration_of_Biogas_Testing_Software.c
This software designed to record data from a
gas-gas membrane separation apparatus.
The processor is a rabbit 2000 on a Wildcat BL2000
motherboard manufactured by z-world. The architecture is
the same as an 8086 based processor.
This software is programmed in Dynamic C++ and uses
ANSI C style programming.
Three pairs of sensors are tied to the A/D board.
One of these is a differential pressure sensor,
one senses the concentration of hydrogen sulfide,
and the other senses the concentration of methane.
The pressure sensor is a Setra Model 264. It works by
converting the deflection of a stainless steel membrane to a
voltage. The effective range of the sensor is 0-1" of water.
It is powered by 12V and its output is 0-12V.
A citi-tech 4HS/LM sensor head is used for sensing the H2S.
The 4HS head is a three terminal sensor attached to a
potentiostat circuit. The three terminals are attached to a
sensing, counter, and reference electrode. The potentiostat
drives the voltage difference between the reference and
counter electrode to 0V. To do this potentiostat must draw
current from the counter to the sensing electrode. The amount
of current it draws is proportional to the concentration of
H2S. A three stage amplifier with an input impedance of
10 Ohm is place between the sensing and counter electrodes.
An MQ-5 sensor put out by Hanwei is used to detect methane.
The sensor is a tin oxide based sensor that varies in
Resistance as the partial pressure of methane increases.
The circuit is a voltage divider using a 5V source.
The load resistance is 470 Ohm.
Copyright 2008 Jerry Martin
North Carolina State University
Biological and Agriculture Engineering Dept.
*/
```

```

// CONSTANTS
    // time between samples (milliseconds)
#define SAMPLE_TIME 500
    //calibration constants
#define PRESSURE_SENSOR_CIRCUIT_GAIN 11.6
#define VOLTAGE_TO_FLOW_CONVERSION_X 147.4
#define VOLTAGE_TO_FLOW_CONVERSION_Y 78.85
//A/D channel that matches each sensor
#define H2S_PERMEATE 2
#define H2S_RETENTATE 3
#define CH4_PERMEATE 7
#define CH4_RETENTATE 4
#define PRESSURE_PERMEATE 0
#define PRESSURE_RETENTATE 1
// boolean values
#define YES 1
#define NO 0
// FUNCTION PROTOTYPES
    // prints time
void Print_Time();
    // reads sensor and returns data
float Read_Sensor(int sensor);
    //samples the flow sensor
void Sample_Flow_Sensor(int adchannel);
    //samples the gas sensor
float Sample_Gas_Sensor(int adchannel);
void main()
{
    // variable declarations
    unsigned long t0 , t1;    // seconds initial, current
    float seconds, time_increment;

// initializations
    brdInit();    //initialize board
    t0 = MS_TIMER;    // zero counter
    time_increment = SAMPLE_TIME / 1000;
                    // calculate sample time in seconds
    //print labels
    Print_Time();
    printf("time, H2SP, H2S R, CH4P, CH4R, FlowP, Flow R\n");
// main program loop
    while (1)
    {

```

```

    costate{}
        costate
        {
            //time samples
seconds += 1;    //increment second counter
            waitfor( IntervalMs(SAMPLE_TIME) );
            // wait for sample time

            // Display the results from the gas sensor
            //measurements
Print_Time(); //print time of measurement
            printf( ",%f," , Read_Sensor( H2S_PERMEATE ) );
            printf( "%f," , Read_Sensor( H2S_RETENTATE ) );
            printf( "%f," , Read_Sensor( CH4_PERMEATE ) );
            printf( "%f," , Read_Sensor( CH4_RETENTATE ) );
            // Read_Sensor(PRESSURE_PERMEATE);
            Read_Sensor(PRESSURE_RETENTATE);
            printf("\n");
        } //end of costate
    } // end while()
} // end main()
void Print_Time()
{
    /* This function prints time */
    unsigned
long the_time; // time variable (seconds since 1980)
    struct tm thetm; // struct for time
    the_time = read_rtc(); //Read the real time clock
    //converts the_time to seconds and fills the time structure
    mktime( &thetm, the_time);
    // prints the time
printf("%02d/%02d/%04d %02d:%02d:%02d",
        thetm.tm_mon, thetm.tm_mday, 1900+thetm.tm_year,
        thetm.tm_hour, thetm.tm_min, thetm.tm_sec);
}
float Read_Sensor( int sensor )
{
    if( sensor == CH4_RETENTATE or sensor == CH4_PERMEATE )
    {
        return Sample_Flow_Sensor( sensor );
    }else
    {
        return Sample_Gas_Sensor( sensor );
    }
}

```

```

    }
}
void Sample_Flow_Sensor( int adchannel )
{
    // variable declarations
    auto int timeout_iteration, i;
    auto float output_voltage, reference_voltage;
    auto float voltage_step_size;
    // initializations
    reference_voltage = 5; // start reference at 5V
    voltage_step_size = 0.25; // start volt step size at 0.25V
    timeout_iteration = 0; // start at 0th iteration
    // begin loop to lock in the reference voltage at
    // a value just below the output voltage
    // timeout at 100 iterations (in case of severe noise)
    while ( timeout_iteration < 100 )
    {
        // set reference voltage
        anaOutVolts( adchannel , reference_voltage );
        // get average of 5 output volt smpls from the pressure
        // circuit
        output_voltage = 0;
        for( i = 0 ; i < 5 ; i++ )
            {output_voltage += anaInVolts( channel );}
        output_voltage = output_voltage / 5;
        // if the output drops to 3.5 V during the sample time
        // (if the output voltage is less than the
        // reference voltage)
        if ( output_voltage < 3.5 )
        {
            // step the reference voltage down
            reference_voltage -= voltage_step_size;
            // if reference voltage is negative something
            //went wrong, break loop
            if (reference_voltage < 0)
                {timeout_iteration = 101;}
        }else
        {
            // increment voltage up
            reference_voltage += voltage_step_size;

            // half the voltage step size
            voltage_step_size = voltage_step_size / 2;
        }
    }
}

```

```

        //timeout if voltage increment becomes small
        if (voltage_step_size < 0.001)
            {timeout_iteration = 101;}
    }
    // increment timeout_iteration
    timeout_iteration += 1;
}
//zero statistics variables
output_voltage_average = 0;
voltvar = 0;
output_voltage_sum = 0;
//sample output voltage 100 times and average
for( i = 0 ; i < 100 ; i++ )
{
    //may need to take break out of the following line
    output_voltage += (anaInVolts( adchannel )
                       / PRESSURE_SENSOR_CIRCUIT_GAIN);
}
output_voltage = ( output_voltage / 100 );
printf( "%f ft^3/min" ,
        ( reference_voltage + output_voltage ) _
* VOLTAGE_TO_FLOW_CONVERSION_X + _
VOLTAGE_TO_FLOW_CONVERSION_Y );
}
float Sample_Gas_Sensor(int adchannel)
{
    // variable declarations
    int i; float sensor_output;
    // variable initializations
    sensor_output = 0;
    // insert small delay to improve accuracy
    for( i=0; i<50 ; i++ ){ }
    // average 50 samples of gas flow data
    for(i=0;i<50;i++)
    {
        sensor_output += anaInVolts(adchannel);
    }
    sensor_output = sensor_output / 50;
    return sensor_output; }

```

APPENDIX E

Another Membrane Configuration?

Much of what was reported in this thesis was discovered through trial and error. In the trial before the experiment reported in the final chapter, it was discovered that the apparatus leaked hydrogen sulfide, but not methane.

The gas was first pressurized at 5 PSI with the retentate valve three eighths of a turn open. At regularly spaced intervals the valve was turned. This choked the flow and forced the gas across the membrane.

The calculated input concentration of the methane equaled the true input concentration of the methane in the biogas when the gas was allowed to run freely past the membrane. This was verified in a duplicate run of the experiment.

When most of the flow passed by the membrane, the estimated input concentration of the biogas came out close to the known concentration. When the flow was forced across the membrane the results were unexpected. The balance on the methane stayed normal, yet some of the hydrogen sulfide was lost.

It is known that polymeric membranes absorb hydrogen sulfide. In this case the gas may have absorbed into the surface of the membrane, and desorbed out every surface of the membrane, including the surface of the membrane left hanging out of the apparatus. Further evidence to support this conclusion were the occurrence of slight deformations under the gaskets along the entire face of the membrane. It was also observed that the entire membrane bound itself to the gasket after the gas desorbed, but could be unbound by exposing it to the gas again.



Figure E.1: Membrane Hanging Out Side of Holder

The loss of hydrogen sulfide through the sides of the apparatus was accidental in nature, however, this may be a different way to use a reverse selective membrane. In the first step of selective diffusion, the membrane absorbs hydrogen sulfide. Since the membrane absorbs across the entire face, it can also desorb across the entire face, including the parts of the face that are external to the apparatus. Methane does not absorb; it must diffuse across the membrane. It has a very long route if it were to diffuse through the sides of the holder, so it must go through the membrane. The porous support structure in the membrane has the pores oriented with the flow, so the gas cannot pass through it sideways. By setting up the membrane with the sides hanging out, the area term in the permeability equation is increased drastically for hydrogen sulfide, but not for methane.

The area of the membrane outside of the holder was estimated at 38 cm² (6 in².) The area available for desorption is twice this because hydrogen sulfide can desorb out of either side of the membrane. Theoretically the hydrogen sulfide lost in this manner would be in a twelve parts lost to one part kept ratio. When the valve was fully closed the hydrogen sulfide was lost close to a nine parts lost to one part kept ratio.

Taking advantage of this, a reverse selective membrane could be engineered into a low pressure forward selective membrane by hanging the sides out of such a holder and allowing the soluble gases to desorb outside of any pipes holding biogas. The waste flow would contain little methane and could be captured and removed. This configuration would be ideal for a biogas system because very little of the methane would be lost.

This apparatus in this experiment was not designed to measure flow leaking from the side of the membrane. Whether or not a sideways configured membrane really works needs to be verified experimentally with a different apparatus.

APPENDIX F

Verification of Maximum Velocity Measurement

A modified setup was used to verify the measurement of maximum flow velocity. In this setup a five foot long , one inch diameter pipe was fastened to the end of the one of the tubes. A two port, six inch, W E Anderson (Dwyer Instruments Inc.) pitot-static (prandtl) tube purchased from Cole-Palmer was placed in the center of the flow and pointed upstream. An Alnor model 560 meter was used to measure the dynamic pressure. To verify the prandtl tube was in the middle of flow, the height of the tube was adjusted until the pressure signal was maximized.

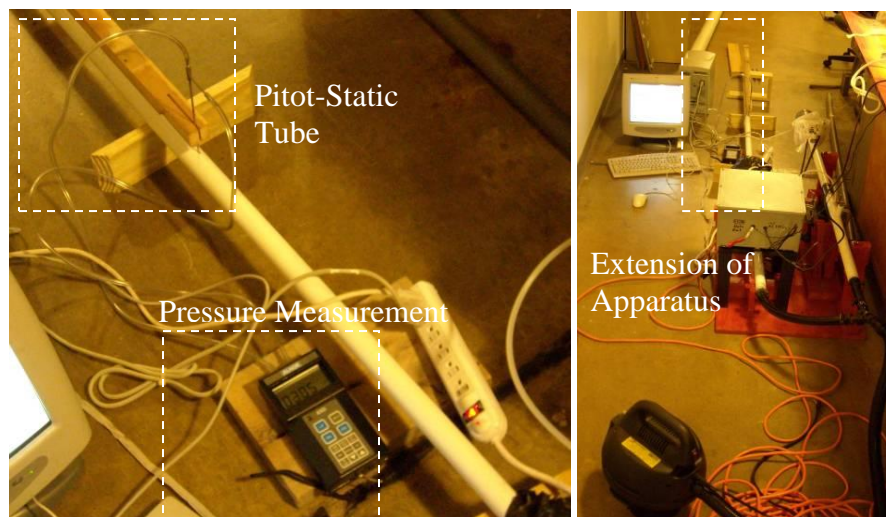


Figure F.1 The Setup Used to Verify the Flow Measurement

The pressure was converted into a velocity according to the instructions included with the pitot-static tube (see Dwyer Instruments Inc. Bulletin no. H-11, 1992). This velocity was graphed in figure F.2 along with measurements from the Sierra 610 velocity meter used in the experiment and against the voltage from the pressure sensors. The two maximum velocity measurements were in agreement.

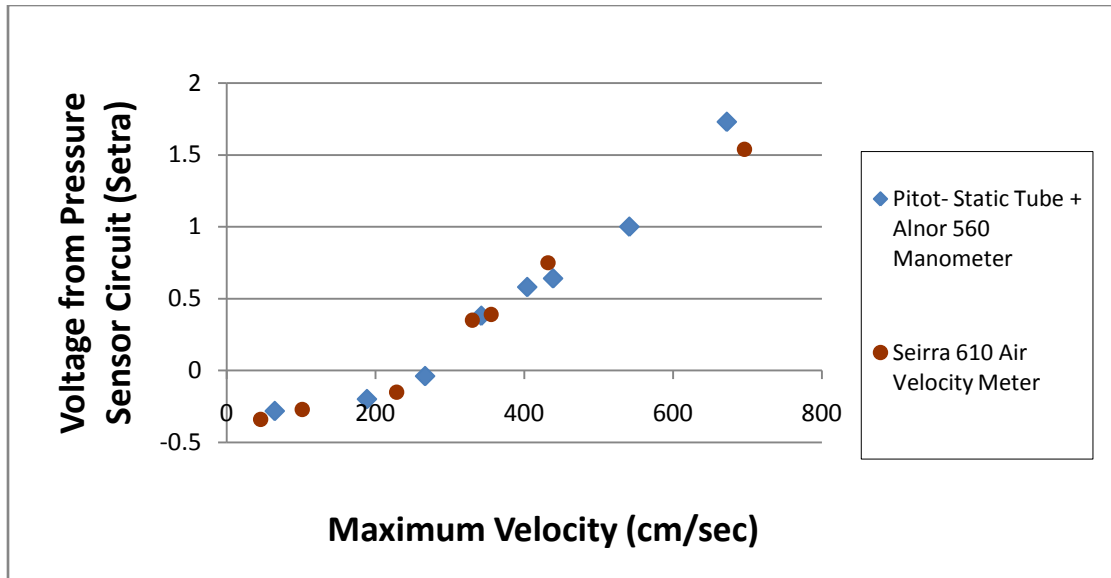


Figure F.2: Comparing the Velocity Measurement in the Experiment to a Second Velocity Measurement Technique

As another check the Reynolds number was calculated. The maximum velocity measured was converted into an effective (mean) velocity by dividing it in half. To calculate the Reynolds number the effective flow was multiplied by the characteristic length (the diameter of the pipe, L) and divided by the kinematic viscosity of air (ν) as shown in equation F.1. The results were graphed in figure F.3.

$$Re = \frac{VL}{\nu} \quad (F.1)$$

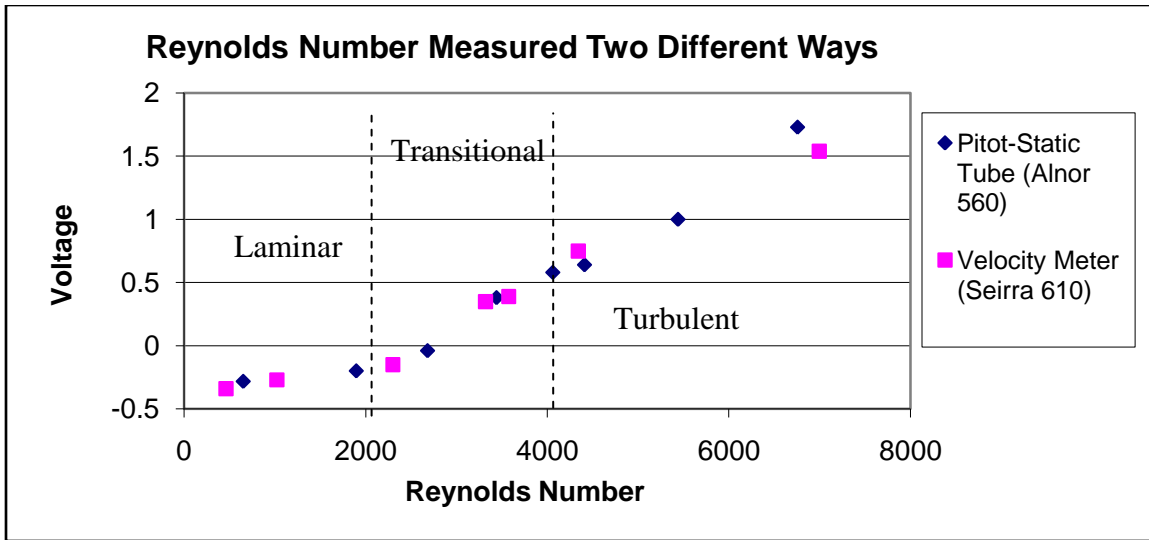


Figure F.3: Figure Showing the Transition from Laminar to Transitional to Turbulent Flow